PeerJ Preprints NOT PEER-REVIEWED

Exploring the occurrence of and explanations for nighttime spikes in dissolved oxygen across coral reef environments

*S.K. Calhoun[1], A.F. Haas[1], Y. Takeshita[2], M.D. Johnson[3], M.D. Fox[4], E.L.A. Kelly[4], B. Mueller[5], M.J.A. Vermeij[5, 6], L.W. Kelly[1], C.E. Nelson[7], N. N. Price[8], T.N.F. Roach[1], F.L. Rohwer[1], J.E. Smith[4]

[1] Department of Biology, San Diego State University, San Diego, CA, United States

[2] Carnegie Institution for Science, Department of Global Ecology, Stanford, CA, United States

[3] Smithsonian Tropical Research Institute, Republic of Panamá

[4] Scripps Institution of Oceanography, University of California San Diego, La Jolla, CA, United States

[5] Caribbean Research and Management of Biodiversity (CARMABI), Willemstad, Curaçao

[6] Aquatic Microbiology, University of Amsterdam, Amsterdam, Netherlands

[7] Center for Microbial Oceanography, University of Hawai‘i at Mānoa

[8] Bigelow Laboratory for Ocean Sciences, East Boothbay, ME, United States

Keywords: coral reef, oxygen budget, nighttime oxygen production, benthic oxygen production, tropical marine systems

PeerJ Preprints NOT PEER-REVIEWED

Abstract

Primary production due to photosynthesis results in daytime oxygen production across marine and freshwater ecosystems. However, a prevalent, globally-occurring nighttime spike in dissolved oxygen (DO) challenges our traditional assumption that oxygen production is limited to daylight hours, particularly in tropical coral reefs. When considered in the context of ecosystem oxygen budget estimates, these nocturnal spikes in DO could account for up to 24 percent of the daytime oxygen production. Here we show, 1) the widespread nature of this phenomenon, 2) the reproducibility across tropical marine ecosystems, 3) the lack of a consistent abiotic mechanism across all datasets we examined, and 4) the observation of nighttime DO spikes *in vitro* from incubations of coral reef benthic samples. Our study suggests that in addition to physical forcing, biological processes may be responsible for the production of oxygen at night, a finding that demands additional research.

Introduction

Canonical light-activated photosynthesis has long reigned supreme as the only biological mechanism that produces significant quantities of oxygen in the atmosphere. Approximately 2.4 billion years ago, cyanobacteria, likely due to their own oxygenic photoautotrophy, evolved to harness a now oxidizing atmosphere by shifting the redox states of carbon compounds (1–3). This ultimately became the cycle of photosynthetic oxygen production and consumption, which is closed when the elementary oxygen generated by photosynthesis serves as a terminal electron acceptor and is converted back to water during aerobic respiration (4, 5). The reduced organic carbons produced during photosynthesis are metabolized by heterotrophic organisms that release CO_2 back into the atmosphere. This balance between photosynthesis and respiration in ecosystems regulates atmospheric carbon dioxide and oxygen concentrations, which in turn affect climate and biogeochemical cycles (6). Between 50% and 85% of the free oxygen produced on Earth is produced by marine photosynthetic organisms (7). While a large fraction of this production is attributed to open ocean phytoplankton, benthic organisms often exceed the productivity of the associated phytoplankton in shallow nearshore systems (8). Other processes producing

oxygen such as oxygenic chemosynthesis have recently been discovered, but these processes contribute insignificant amounts of extracellular free oxygen to the global oxygen budget (9, 10). Therefore, the significance of photosynthesis, especially when constructing ecosystem and global oxygen budgets cannot be overstated, nor the potential contribution of marine benthic organisms (e.g. the seafloor inhabitants of the world's coral reefs) to those budgets.

To quantify ecosystem metabolism in tropical coastal environments, studies historically measured benthic community production using flow respirometry (e.g., Odum, 1957; Kinsey, 1985; Kraines et al., 1996) or incubation experiments (e.g., Sournia, 1976; Kraines et al., 1998). These studies significantly added to a general understanding of the photosynthesis-respiration equilibrium. However, they frequently lacked the temporal resolution (a few measurements per day versus one measurement every few minutes) and extended duration (a single day versus multiple consecutive days to months) that facilitates the discovery of underlying ecological drivers which are often observed in long-term data trends and anomalies. Progress toward resolving this issue was achieved with the development of autonomous dissolved oxygen sensors (e.g., electrodes and optodes) and associated data loggers that have produced numerous high-frequency *in situ* oxygen measurements in recent decades. Extensive dissolved oxygen (DO) time series data are now available for shallow near-shore environments around the world (16–18). The analysis and interpretation of these time series data sets can be complex because *in situ* DO concentrations depend on a multitude of known (e.g., light availability, hydrodynamics, biofouling) and unknown influences (19). Consequently, certain characteristics of these time series that are not well understood have remained unexplained in any detail, if at all.

One particular feature of many DO time series from coral reefs and to a lesser extent other shallow, near-shore marine systems around the globe is a distinctive, pulsed increase in DO concentration at night, equivalent to as much as 24% of the daytime oxygen production. Because it is generally accepted that oxygen production in the marine environment can only occur in the presence of photosynthetically active radiation (PAR), these nighttime spikes are presumed to be attributed to physical processes such as

tidal bores, groundwater intrusion, upwelling, mixing, or thermal stratification in the water column. In this context, these DO spikes are no less significant to the overall oxygen budget than if they were biological in origin. An allochthonous (outside the system) input of oxygen, regardless of origin, will skew any estimate of ecosystem respiration that relies on measurements of oxygen consumption. Since the DO spike at night is omitted in the classical view of oxygen production during the day, it is often excluded as an input, leading to an underestimate of the actual amount of oxygen consumed. Additionally, we have been accumulating evidence of a possible biological source for these spikes in tropical benthic communities over the last five years. We concluded there is a need to further investigate the worldwide occurrence of this phenomenon by teasing apart physical and biological processes that may be responsible. Here we use rigorous review of literature, *in situ* DO time series, incubation experiments *in situ*, and controlled laboratory experiments to determine that these patterns are widespread, frequent, and difficult to explain with any single physical or environmental variable. Furthermore, nighttime spikes in DO were observed under isolated laboratory conditions, strongly indicating a potential biological origin that may contribute significantly to the global oxygen budget.

Results

Review of the Literature

An extensive search of the literature identified 28 (20 temperate, 8 tropical) studies that have published DO time series datasets spanning 24 hours or more between 1970 and 2015 (See Methods for search and selection parameters). Including an additional 13 datasets presented here, 78% (32 out of 41) document an increase and subsequent decrease in DO concentration during the night lasting between 4 and 8 hours, with 63% (20 out of 32) of those studies originating in the tropics (Figure 1, Table S1). Quantitative comparisons across these datasets are difficult due to the different reported DO units (e.g. percent air saturation, µmol L^{-1}, mg L^{-1}, mmol m^{-2} d^{-1}), and calculating DO values for each using a consistent metric would require access to numerous unpublished datasets. However, many useful qualitative details can be observed in the published figures and data. Two studies on the Island of

Mo'orea (14, 20) (Figure 1, inset numbers 29-30) identified a nighttime DO spike, but did not discuss the observation. Hydrodynamics was suggested to cause nighttime variability in DO off the coast of Japan by way of currents bringing more oxygenated offshore water onto the reef (21) (Figure 1, number 12 inset). Evidence in support of this hypothesis includes shifts in pH, temperature, and tides that occurred simultaneously with the DO spike indicative of changing hydrodynamic conditions on the study location.

Methods can indicate whether the DO increase results from physical or biological processes. Because argon's dissolution properties in seawater are very similar to those of oxygen, changes in oxygen:argon ratios (δO_2:Ar) can be used to distinguish between biologically produced DO increases and atmospheric dissolution of DO. Luz and Barkan (2009) used this method to calculate net oxygen production in the Red Sea (Figure 1, number 7 inset) and showed a spike in δO_2:Ar between 01:00 a.m. and 05:00 a.m., which supports biologically derived net oxygen production at night. These studies illustrate that the origin of DO spikes has been attributed to both biological and physical processes, but also that they are often simply ignored. Nevertheless, the observation of a spike in DO at night in numerous published datasets appears to be a common phenomenon across the tropics, though the underlying mechanisms have never been specifically investigated.

Repeatability of Nighttime Oxygen Production *in situ*

Our *in situ* datasets in this study represent autonomous multi-sensor sonde (hereafter referred to as 'sensor') deployments across the central Pacific and Caribbean basins spanning the years 2010 - 2015. DO datasets were obtained from enclosures deployed during Sept., 2011 on the island of Mo'orea, French Polynesia using sensors inside collapsible benthic isolation tents (cBITs - Figure S1, after (23)). Between three and five sites on the back reef of Mo'orea were monitored for 48 hours during five separate cBIT placements, with continuous DO and temperature measurements recorded every 15 minutes. A similar method was carried out during 2010 and 2013 in the Line Islands (11 islands stretching 2,350 km northwest-southeast across the equator), where cBITs were simultaneously placed at six fore-reef sites around each island (Kingman, Palmyra, Washington, Fanning and Christmas during Oct.-Nov., 2010;

Jarvis, Malden, Starbuck, Millennium, Vostok and Flint during Oct.-Nov., 2013). Measurements were logged for one deployment of 36 hours, again at 15-minute intervals. No dataset from Christmas Island was used in our analysis due to inclement weather conditions there that prevented reliable data collection.

In situ DO and temperature surveys (i.e, sensor deployments where no enclosure was used at any point) were taken during Sept., 2014 on the fore-reef of Palmyra Atoll in the northern Line Islands (24), and during May, 2015 on the fringing reef slope of the island of Curaçao in the southern Caribbean. An additional dataset included in this analysis was derived from an *ex situ* survey during Aug., 2014 of an artificial tropical reef environment at Birch Aquarium at the Scripps Institution of Oceanography, San Diego, CA, USA to serve as an example of nighttime DO spikes that are removed from an open ocean environment, yet still subject to external physical influences such as atmospheric temperature changes and moving water masses (see Methods for description). Surveys lasted three or more consecutive days (Palmyra, 15 days; Curaçao, 5 days; Birch Aquarium, 3 days) with a measurement interval of 15 minutes. We observed nighttime DO spikes (defined as a DO concentration increase in the absence of PAR, lasting at least two hours before decreasing again) across all our datasets for a total of 63 nights where they occurred, showing DO spikes happening during 77% of all surveyed nights (82 nights in total) (Figure S2).

Initial Assessment of Potential Mechanisms

To test potential physical mechanisms for these nighttime spikes, we utilized a suite of *in situ* data collected concurrently with DO. The simultaneous change of various oceanographic parameters such as temperature, salinity, current direction and current speed can indicate whether or not a DO spike coincides with changes in the overlying water mass (21). Therefore we analyzed our own datasets to assess whether nighttime DO spikes coincided with temperature spikes of a similar magnitude and duration (Figure 2). The most comprehensive dataset used for this analysis originates from an *in situ* survey of Palmyra Atoll in the Northern Line Islands (24) consisting of simultaneous measurements of DO, temperature, pH, current speed and current direction that were taken every 15 min over 15 days at

two separate sites ('LL' and 'RT4'). During this survey, a total of 21 nighttime DO spikes were observed, of which 62% (13 spikes) coincided with a concurrent spike in temperature (Figure S3). In all other cases DO spikes coincided with a shift in current speed, current direction, or both (excluding two instances where no simultaneous current data were recorded). Simultaneous shifts of all measured oceanographic parameters during DO spikes were rare and occurred only twice.

Across all *in situ* data, temperature spikes co-occurred with nighttime DO spikes 37% of the time and only at sites in 10 m water depth in fore-reef habitats of the central Pacific Islands. While turbulent wave action typical for fore reef-sites across the Line Islands certainly contributes to local changes in DO concentrations, locations with less intense water movement (i.e., back reef habitat on Mo'orea, Curaçao, and especially the Birch Aquarium reef tanks) all exhibited nighttime DO spikes that could not be correlated with water movement.

Statistical Analysis of Potential Mechanisms

We employed multivariate Granger causality analysis on unfiltered time series data to elucidate independent physical variables that might influence the nightly spikes in DO concentrations observed across our study sites. This analysis allowed us to assess distant influences across multiple time series parameters and to determine their predictive value (25). Parameters that covary with DO in our time series data did not provide any means of predicting future changes in DO, such as the repeated occurrence of nighttime DO spikes, and were detected as bi-directional predictions (Table S2). Birch Aquarium is a fully indoor facility with no natural light, therefore we excluded this dataset in our analysis here.

Analysis of DO time series for deployments in the back reef of the island of Mo'orea did not identify any one physical predictor of the DO measurements across all sites and sensors deployed (Table S3, Mo'orea). However, wind speed was found to either covary or predict DO during two out of the five cBIT deployment rounds (Table S2, Mo'orea). Covariance between wind speed and DO is not surprising for Mo'orea, as previous research has shown that wave action and wind speed drive water transport across

the back reef (26). Yet observation of Mo'orea's back reef retention times combined with evidence against groundwater flow indicate that the cBITs deployed during this study had internal retention times on the order of hours if not days, effectively decoupling them from the surrounding bulk water transport (27, 28). The nearly identical amplitudes of the nighttime DO spikes between two datasets, one with wind as a predictor and one without (Figure 3A and 3B) support the conclusion that wind did not affect the nighttime DO spikes inside the cBITs at Mo'orea.

During the cBIT deployments in the Line Islands, the overall DO patterns recorded by all six sensors at each island showed very little variation between the sensors, leading to the conclusion that oxygen production and consumption was relatively homogenous. Therefore, when assessing the influence of any variable over DO, only variables that showed a significant predictive value across all six sensors were considered meaningful. Only two islands show correlations between all six sensors' data and a physical parameter (Table S3, Flint – wind speed, Millennium – moon phase).

Comparing the average amplitudes for the nighttime DO spikes between Millennium (an island with a predictor of DO) and Starbuck (an island without any predictor) shows that amplitudes vary substantially between the two islands (Figure 3C and 3D). A 5 µmol kg^{-1} amplitude DO spike occurred on Starbuck (Figure 3C, Table S3), yet a DO spike of 15 µmol kg^{-1} in amplitude was recorded on the reefs of Millennium, related to the moon phase (Figure 3D, Table S3). Maximum moon illuminance during the Millennium deployment ranges from 0% (new moon) to 8% (waxing crescent) over November 5^{th}-8^{th}, 2013. During the Starbuck Island deployment, maximum moon illuminance moves from 60% (waning gibbous) to 32% (waning crescent) across October 26^{th}-30^{th}, 2013. This pattern shows that moonlight intensity is unlikely to be related to DO concentration in this system.

Higher tidal amplitudes associated with spring tides, align with the new and full moon. This provides a logical explanation for moon phase being a predictor of DO spikes during the new moon on Millennium island, where tidal forcing and subsequent tidal bores would be more extreme. While the enclosed mesocosm design of the cBITs may have mitigated effects from the immediately overlying

water mass, it was not possible to fully seal the chambers on the porous, extremely rugose reef benthos. Therefore, an increase in the amplitude of nighttime DO spikes during an increase in tidal force is possible, but the occurrence and frequency of the nighttime DO spikes does not directly associate with tidal patterns across our entire data set as evidenced by the lack of moon phase as a predictor of DO in a majority of cases.

Additional deployments of autonomous sensors (without cBITs or other enclosures) for longer periods of time were carried out on Palmyra Atoll in the central Pacific (24) and Curaçao in the Southern Caribbean. These data show nighttime DO spikes across different sites over several days approaching upwards of 15 µmol kg^{-1} for Palmyra (Figure 4A) and 2 µmol kg^{-1} for Curaçao (Figure 4B). No physical variable (wind, tide, moon phase) was found to have any predictive power over the DO spikes for Curaçao. Pressure changes near the benthos from directional current changes predicted the DO concentration at site RT4 at Palmyra (Table S3, Palmyra 2014).

Surprisingly, neither current speed nor current direction was found to predict DO for either site LL or RT4 at Palmyra. It is possible that changes in current speed on Palmyra were too stochastic in amplitude and frequency to be statistical predictors of changes in DO. However, changes in current direction for both sites do not appear as stochastic in nature (Figure S3). The lack of any statistical significance here is perhaps due to the representation of polar coordinates as a linear time series. Intuitively a polar coordinate time series is represented as a flattened cylinder, creating an artificial gap between continuous measurements. This gap may have thrown off a reliable comparison of these data to a DO time series. In light of this shortcoming, pressure serves as a reasonable proxy and further verifies the previous observations of current direction and DO in this data. Pressure was a predictor of DO for site RT4, where a change in current direction always coincides with nighttime DO spikes. Pressure was a co-varying parameter at site LL (Table S3), where a change in current direction frequently coincides with nighttime DO spikes.

In sum, we identified a number of physical parameters that, in a minority of cases, explained the amplitude or frequency of nighttime DO spikes observed on coral reefs, albeit on a rather variable and site-specific level. Given the propensity of nighttime DO spikes one would expect more consistent physical correlations between DO spikes and physical factors. While it is obvious that physical forces influence DO concentrations during the night on reefs, our data do not suggest that abiotic mechanisms are wholly responsible for their existence. The presence of nighttime DO spikes in an artificial system (e.g. Birch Aquarium – Figure 4C) demonstrates that these spikes can even occur outside of an oceanographic context and motivated further study in a laboratory setting.

Laboratory Incubations

To identify what, if any, contribution from benthic organisms exists in the nighttime DO spikes, we conducted a series of studies at the CARMABI research station on Curaçao during 2015 and 2016. In 2015, multiple benthic substrate types representing turf forming algae ('turf'), sediment, calcium carbonate rubble ('rubble'), crustose coralline algae ('CCA') or a mixture of many indiscernible substrates ('mixed') from various reef sites were incubated for 12-hours in the dark (Figure S4, see Methods for details). A DO spike was defined as an increase in DO concentration with an amplitude equal to or greater than 50 µmol kg^{-1} that lasted for >1 hour. This threshold represents the maximum amplitude recorded *in situ*, and was chosen so that any observation of a DO spike could be considered relatively equivalent to those seen on a coral reef. Nighttime DO spikes exceeding 50 µmol kg^{-1} were only seen in incubations with CCA, where spikes were measured between 60 – 100 µmol kg^{-1} (Figure 5A, Table S4). Lower amplitude spikes (between 10 and 25 µmol kg^{-1}) were observed for other benthic communities (Figure S5 - C, E and F). This could indicate the involvement of a complex community of organisms, where CCA is a key player. Overall the contribution of CCA to the DO spikes could be explained as either sufficient but not required due to the presence of smaller DO spikes in non-CCA incubations, or necessary in such a way that an imperceptible amount of CCA (or microorganisms associated with CCA) could be responsible. The lack of any DO spikes seen in incubations of sediment samples supports the

latter hypothesis: a small amount of CCA or CCA-associated microbes could be present underneath turf, inside rubble and in mixed benthic substrate types, but is less likely in a predominantly sediment substrate.

To further isolate possible drivers of the DO spikes and the relationship seen with CCA, additional incubations were performed in 2016. During these incubations, much less biological material was introduced into the incubation chamber (10 – 20 mL of pulverized CCA slurry as opposed to 200 – 500 mL of intact CCA), and the amplitude threshold for determining a significant DO spike was reduced to equal to or greater than 15 µmol kg^{-1} (the lower end for recorded DO spikes *in situ*). CCA samples collected from across the island were separated into epilithic (the first ~1 mm of crushed surface material) and endolithic (crushed inner core material) communities, and five samples of epilith and two of endolith were incubated for two days. We observed a 17 µmol kg^{-1} nighttime DO spike from one epilithic sample, and none from any endolithic sample (Figures 5B and S6). Because high amplitude DO spikes occurred irregularly and we were unable to link specific organisms to the DO spikes, CCA samples were transported to San Diego State University, San Diego, CA for further study (see Methods). After approximately one week of acclimation, intact CCA samples from 2015 were monitored with the same sensors used in Curaçao, and a DO spike approaching 50 µmol kg^{-1} in amplitude was observed in complete darkness (Figure S7A).

Assessment of Oxygen Budget Deficits

Considering the prevalence of the nighttime DO spikes at both and ecosystem and organismal levels, we wanted to quantify a subset of these instances to demonstrate the significance of their omission from oxygen budget calculations. Using a rough estimate of the integrated daytime DO production and nighttime DO spikes for a representative 24-hour period in datasets presented here, we find an estimated 4 - 24% of oxygen input is not accounted for when ignoring nighttime DO spikes (Figure 6). This represents either an underestimate of respiration at night, an underestimate of net oxygen production, or some combination of both.

Discussion

Here we provide unequivocal evidence that nighttime DO spikes occur regularly on the coral reef benthos around the world. We used a combination of peer reviewed, published data from 1970-present, our own field-based data collected from two ocean basins and data collected in controlled laboratory settings to corroborate these findings. In addition to documenting the existence of nighttime oxygen spikes in the environment, we sought to identify potential causal mechanisms. After extensive analyses of a variety of physical, environmental and oceanographic predictor variables, we were unable to definitively identify one consistent explanatory variable or set of variables. Further, detailed laboratory studies under controlled conditions allowed our team to isolate the pattern in a closed system, suggesting that DO spikes are likely the results of a biological, rather than a physical, process. These findings have important implications for the calculation of oxygen budgets around the world, and suggest that previous studies may have significantly underestimated net oxygen production by not considering the nighttime oxygen influx (Figure 6).

It is tempting to explain these nighttime DO spikes as the slowing of community respiration rate based on the general trend of a relatively high daytime respiration rate continuing for a few hours after sunset, then slowing significantly. However, this could only potentially explain a slowing or cessation of oxygen consumption. In order for DO to increase there must be either autochthonous oxygen (e.g. biological production *in situ*) or allochthonous oxygen inputs (e.g. transport by physical processes such as tides, currents or wind-driven waves), both of which have been addressed in this study. Across the suite of potential physical explanations for the nighttime DO spikes, none truly fit with our observations. Purely abiotic processes, even the effect of several different physical processes unique to each instance of a DO spike, cannot conclusively explain the results of our laboratory incubations where we show that DO spikes occur in an effectively lightless, temperature controlled, isolated environment (Figure 5A and 5B).

While calculations of oxygen budgets for any ecosystem focus almost exclusively on PAR-driven photosynthesis, other candidates for biological oxygen production have recently been proposed.

289 Specifically, oxygenic chlorite detoxification by perchlorate-respiring bacteria and oxygenic nitrite
290 reduction by the recently identified bacterium *Methylomirabilis oxyfera* (9, 10) have been documented.
291 Far-red light photosynthesis has also recently been documented in cyanobacteria as an adaptation to
292 extremely low light environments (29). However, these explanations do not logically explain the
293 occurrence of nighttime DO spikes near the benthos of an oligotrophic coral reef at depths that filter out
294 long wavelengths of light, including far-red light. Reactive oxygen species detoxification can also
295 regenerate molecular oxygen from oxygen radicals and hydrogen peroxide generated during aerobic
296 respiration (30). While we have no evidence that this or any other mechanism is specifically involved in
297 nighttime DO spikes, these examples do show that biological processes capable of releasing oxygen in the
298 absence of sunlight exist.

299 Our research highlights the possibility that a previously undescribed oxygenic biological process
300 may be at work here, and more importantly that patterns of DO in nature are more complex than
301 previously appreciated. These findings have important implications for biological feedbacks, benthic
302 boundary layer dynamics, hypoxia, reef metabolism and overall coral reef health and resilience. The
303 production of oxygen at night may prevent hypoxia from occurring within the reef interstices and on the
304 benthos, and may influence the physiology of the diversity of taxa inhabiting reef ecosystems. Based
305 upon extensive analyses, we found no clear and consistent physical driver(s) of these patterns suggesting
306 that the causes are variable or may be the result of some as of yet uncharacterized biological process.
307 Given the novelty of these findings and the potential importance of the results for calculation of global
308 oxygen budgets, we hope that these results motivate future research to help resolve this widespread and
309 ecologically important phenomenon.

310 ## Methods

311 ### Review of the Literature

312 We performed an extensive search of the literature to determine the prevalence of nighttime
313 spikes in dissolved oxygen (DO) from published *in situ* time series datasets. In total we reviewed >3000

papers using ISI Web of Science, Google Scholar, and the University of California San Diego Research Data Collections (http://library.ucsd.edu/dc/rdcp/collections) with the keywords 'coral oxygen', 'marine nighttime oxygen', 'marine oxygen', 'aquatic oxygen', and 'marine calcification' with publication dates between 1970 and 2015. Up to the first 1,000 publication hits for each keyword phrase were screened for figures of *in situ* DO time series plots with three or more consecutive time-point measurements per night spanning at least 24 hours. After identifying plots that met our criteria, we distinguished nighttime DO spikes in those plots as DO concentration increases in the absence of PAR, lasting at least two hours before decreasing again. In total, 28 (20 temperate, 8 tropical) datasets were singled out, where 19 showed an increase and subsequent decrease in DO at night generally lasting 4-6 hours (Table S1).

Datasets

To determine if nighttime oxygen production was predictable and found across reefs and habitats, we conducted a series of *in situ* studies from three coral reef environments within the Central Pacific Ocean and Caribbean Sea between 2010 and 2015: The Line Islands (Central Pacific), Mo'orea (French Polynesia), and Curaçao (Southern Caribbean).

Mo'orea 2011

Sites at the island of Mo'orea (17°48'S 149°84'W) were monitored from September 1 through 22, 2011. Collapsible benthic isolation tents (cBITs – Figure S1) were deployed for 36 hours at 5 m depth on the back reef habitat of Mo'orea for the purpose of isolating the benthic water column from the surrounding seawater, after the methods described by Haas et al., (2013).

Line Islands 2010 and 2013

The Northern Line Islands consist of 5 individual islands spanning latitudes from 6°24'N to 1°53'N in a northwest to southeast trend. Atoll and fringing reef structures dominate the marine terrain around each, consistent with the whole of the Line Islands chain. Research was conducted across these islands from October 24 to November 23, 2010 using the cBIT setup previously described, with a mean

daily PAR measurement of 328 +/- 175 umol photons m^{-1} s^{-1} and water temperature of 26.5 +/- 1.3^{o}C (collected at 15 min intervals using a LICOR [LI-COR, Inc., www.licor.com] and a MANTA multiprobe sonde [Eureka Water Probes, www.waterprobes.com)] respectively). The Southern Line Islands are an additional 6 islands of the Line Islands chain spanning 0°22'S to 11°26'S, making the whole of the Line Islands one of the longest island chains in the world (2,350 km from north to south). Research studies were conducted across these islands from October 18 to November 6, 2013, with a mean daily PAR measurement of 312 +/- 214 umol photons m^{-1} s^{-1} and water temperature of 28.1 +/- 0.5^{o}C (collected as described for the Northern Line Islands). cBITs were deployed at 10 m on the fore-reef habitat in all the Line Islands (6 per site, across 11 islands).

Palmyra 2014

A single island research study was carried out from September 8 to 24, 2014 on Palmyra Atoll, the second northernmost island of the Line Islands (5°52'N 162°6'W) as described by Takeshita et. al. (2016)(24).

Curacao 2015

The island of Curaçao (12°7'N 68°56'W) is located approximately 64 km northeast of the Venezuelan coast on the southernmost edge of the Caribbean tectonic plate. It is a semi-arid island surrounded by fringing reefs, with greater coral diversity and coral coverage than much of the Caribbean(31). Research on this island was conducted out of the CARMABI Research Station from April 14 to May 28, 2015. A mean temperature of 26.7 +/- 0.1^{o}C was collected as described for the previous islands. A single MANTA multiprobe sonde was deployed in Curaçao at 10 m of depth approximately 200 m offshore of a desalinization plant located at 12^{o}6'N, 68^{o}57'W. The MANTA was set up to autonomously log parameters per the deployment for Mo'orea and the Line Islands, with the exception that no cBITs were used.

Birch Aquarium 2014

In addition to field deployments, water chemistry in the coral reef tanks at the Birch Aquarium at Scripps Institution of Oceanography (University of California San Diego, San Diego, CA, USA) was monitored over August 8-18, 2014. All data were collected using MANTA multiprobe sondes as per other field studies described here. A total of five aquaria labeled tank 26, 27, 31, 15a and 15b were observed using six MANTAs: one in each tank, except for tank 26 where two MANTAs were placed, one in a relatively high flow location and one in a lower flow location. This was done because of the more variable flow pattern in tank 26 (see Table S5 for a summary of flow rates and other metrics for each aquarium).

No aquaria are aerated via pumped air, and instead rely on water pump rates and flow schemes to provide water aeration. The filtration and flow scheme for each tank number is as follows:

Tank 26.

1. A pump draws water from the sump and is sent through a 2-way pneumatic valve controlled by a timer, which switches direction to spray bars located on either end of the tank. Every 5 minutes water flow direction changes.
2. Water from the tank drains through a weir box, by gravity, and flows into 4, 100 µm filter socks located at one end of the sump.
3. Water then travels through two baffles and into the next section of the sump. Here, a submersible pump sends water to a protein skimmer also located in the sump. The protein skimmer drains back into the sump.
4. The cycle starts over again. Filtered seawater from Scripps Pier ran continually at about 1 L/min through a 25 µm pleated filter before flowing into the sump, creating a 25% water change per 24 h.

Tank 27.

1. A pump draws water from the sump and is sent through a 2-way pneumatic valve controlled by a timer, which switches direction to spray bars located on either end of the tank. Every 5 minutes water flow direction changes.

PeerJ Preprints NOT PEER-REVIEWED

2. Water from the tank drains through a weir box, by gravity, and flows into 1, 100 µm filter sock located at one end of the sump.
3. Water then travels through two baffles and into the next section of the sump. Here, an external pump sends water to a protein skimmer located on top of the sump. The protein skimmer drains back into the sump.
4. The cycle starts over again. Filtered seawater from Scripps Pier runs continually at about 2 L/min into the tank and sump.

Tank 31.

Natural seawater flows directly into tank and drains out. No external filtration or chemical additives.

Tanks 15a and 15b.

Both are connected to one sump. Tank 15a is a long tank with a divider, where the shorter section is the sump. A submersible pump in this sump provides flow to both tanks. Tank 15b sits 0.5 m away from 15a, and they run parallel to each other. Water drains from both tanks through an overflow drain located at one end of 15b.

All tropical aquaria use seawater drawn from 3 m below the surface at nearby Scripps Pier into a reservoir before being heated and pumped into each tank. Seawater flows, by gravity, down a flume along the side of the pier into a settling pit where large items settle to the bottom. It is then pumped through a sand filter (silica sand #20 grade) and to a 227,000 L reservoir near the pier. From the reservoir, it is pumped up a hill to another 227,000 L reservoir that sits uphill from the Aquarium in order to facilitate a gravity fed flow to the aquaria. When the seawater arrives at the Aquarium some of that water is diverted to a warm water reservoir where it passes through a 100 µm filter sock, gets warmed to 23^{o}C, and then pumped to tropical aquariums.

Tanks 26, 27 and 31 were set up as display tanks with tropical vertebrate and invertebrate species including corals present. Tanks 15a and 15b were not display tanks, but instead housed numerous coral and CCA species for future display tank placement and at a greater density than the display tanks.

Statistical Analysis of Datasets

All time series data were analyzed using MatLab (R2015a, MathWorks, Inc.). DO concentration in μmol kg^{-1} was calculated from percent saturation, temperature and conductivity measurements using functions from SEAWATER Library v. 3.3 (http://www.cmar.csiro.au/datacentre/ext_docs/seawater.htm) and Gibbs Seawater Oceanographic Toolbox (http://www.teos-10.org/pubs/gsw/html/gsw_contents.html). Data were normalized to the overall average of the first 30 min of all six sensors in the Line Islands deployments (cBITs).

Temperature to DO comparisons were made using smoothed (low-pass filter, window = 6 h, order = 5) time series data. A temperature spike was considered to covary with a nighttime DO spike if the peak of the temperature spike occurred at the same time or within the preceding hour of the DO spike.

Multivariate Granger causality analysis was carried out using the MVGC toolbox (25) on unfiltered data. Bayesian information criteria was used to estimate a vector autoregressive model order, followed by pair-wise covariance estimation using ordinary least squares regression. Statistical significance for each pair was determined by an f-test with a p-value threshold of 0.05

For lab based studies during 2015, an amplitude threshold equal to or greater than 50 μmol kg^{-1} and a duration threshold >1 hour was used to determine the point at which a DO concentration spike could be considered significant. These thresholds represent the most pronounced observations of *in situ* nighttime DO spikes from the Line Islands and Mo‘orea sites. Any fluctuations in DO concentration measurements during the lab incubations that fell below these thresholds were counted as negative for nighttime DO spikes (Table S4 and Figure S4). For the 2016 studies, the amplitude threshold for determining a significant DO spike was reduced to equal to or greater than 15 μmol kg^{-1} (the lower end for recorded DO spikes *in situ*).

Physical and meteorological data used in GC analysis

NOAA weather buoy data (http://www.ndbc.noaa.gov) from buoys stationed at 155°W and 8°N-8°S over the dates listed for Northern and Southern Line Islands cBIT deployments was used to obtain

pressure at 300 and 500m of seawater depth, as well as wind speed. Moon phase, temperature, humidity, atmospheric pressure, wind speed, and wind direction data from a combination of local airports, NOAA, and personal weather stations (http://www.wunderground.com/about/data.asp) was used for all sites where buoy data was unavailable.

Laboratory Incubations

To determine if nighttime DO spikes observed *in situ* could be isolated in the laboratory, several different benthic components were collected from the reefs of Curaçao and brought into the lab during April-May, 2015. Benthic components included five basic types: fine grained sand/sediment ('Sediment'), rubble covered in turf algae ('Turf'), bare limestone rubble ('Rubble'), crustose coralline algae ('CCA'), and mixed benthic communities where no benthic component comprised more than 25% of total ('Mixed') (See Table S4 for a list of all samples incubated). Sample composition was determined by visual assessment of the surface area of the sample, where the sample was classified as one of the five types per the dominant (>75% of surface area) sample type present.

Incubation tanks were constructed using a transparent polycarbonate tube design, with rubber gasket sealed lids on either end. Tubes were oriented vertically with a sealed port on the bottom lid and open top for access by the sensors. Multiple sensor types were deployed to measure dissolved oxygen and temperature during the incubations. These included MANTA multisensor sondes, a single-channel fiber-optic oxygen sensor (PreSens Precision Sensing GmbH, www.presens.de) combined with a HOBO temperature logger (HOBO Pendant Temperature/Light 8K Data Logger, Onset Computer Corp., www.onset.com), and a handheld optical sensor set to continuously log measurements (HACH HDQ Portable Meter with optical DO sensor, HACH Company, www.hach.com). Each incubation tank held a volume of approximately 2 L of seawater, and measured 7.5 cm in diameter by 50 cm tall. The tanks were installed in a temperature controlled water bath that was placed in a temperature-controlled room (24 +/- 0.5 ^{o}C). PAR measured inside the water bath showed 0.0 μmol m^{-2} s^{-1}, an effectively lightless environment. No external or internal water flow was allowed in any tank during the incubation period in

order to minimize the possibility of introducing external DO. Additionally, the surface area of the seawater inside each tank exposed to air was minimized as best as possible by the position of the sensors at the top and vertical orientation of each tube, blocking direct seawater-air contact.

Benthic samples comprising the five basic types listed were collected from varying depths at several locations across the island of Curaçao (Table S4). All samples were collected in polycarbonate incubation tubes filled with ambient seawater, sealed and transported to CARMABI where they were immediately transferred to new incubation tubes filled with seawater from the flow-through system and placed in the incubation chamber, except for certain CCA samples. CCA samples from deeper than the intertidal zone were allowed to recover for 48 hours in a low-light aquarium with flow before incubation in order to minimize the stress of being chiseled off the reef during collection. No other samples were collected by chiseling. Differing amounts of biomass as determined by volumetric displacement were incubated for each sample type to determine if the nighttime DO spikes occurred due to a specific amount of biomass. Samples were either incubated in singlet, duplicate or triplicate depending on the amount of sample available. A total of four control samples were incubated: a tap-water control to check the abiotic DO to temperature correlation, a water column control collected from the reef at 10 m depth and a water column control from the surface water to observe the DO variability in the water column alone, and dry rubble exposed to direct sunlight for 12 hours then submerged in seawater to observe the DO variability of rubble removed from a typical reef system (Figure S4A).

Incubations were carried out over a 12-hour period for all samples, with individual incubations designated by number. A numbering scheme of ‘0.00’ was used, where the number in front of the decimal designates the arbitrary sample number of an individual sample (reset for each round of incubations), and the number after the decimal indicates the incubation round (numbered continuously). After each incubation, crustose coralline algae (CCA) samples were placed in either an open plastic bowl in a low-light aquarium with seawater flow (samples from >5 m), or a polycarbonate incubation chamber with all ports open anchored in the intertidal zone in front of CARMABI. The CCA samples were allowed to

recover for a minimum of 24 hours to ensure sample survival for ongoing incubations. All other samples were subsampled after incubation into a 50 mL conical tube, frozen at -80°C for later nucleic acid extraction, and the remainder discarded.

A similar incubation setup was used during the incubation experiments carried out at CARMABI over April-May, 2016 (Figure S5). Incubation chambers were of the cylindrical polycarbonate tube design, but could be fully sealed using custom lids that allowed either a fiber-optic optode (PreSens) or a multisensor sonde (MANTA) to be placed in a fitted port in the lid. Total chamber volumes were 1 L for the chambers using a PreSens optode and 1.5 L for those using a MANTA array. This was done to help compensate for the displacement of the relatively large MANTA array compared to the thin fiber-optic optodes. The incubation chambers were placed in a water bath covered with a tent of light-blocking fabric over a PVC frame. Aquarium lights on a digital timer were attached to the inside of the PVC frame, allowing for simulation of a controlled diurnal cycle that mimicked the sunrise and set times for the area. The entire water bath and tent setup was stationed in a climate controlled room, where temperature inside the water bath was maintained at 23.0 +/- 0.2 ^{o}C.

CCA samples were collected from various sites around the island of Curacao at depths ranging from 0.5 – 15 m and held in a shaded aquarium with flow until processing and incubation. Processing to generate CCA slurry was carried out using a steel chisel to gently chip away an approximately 1 mm deep layer of the surface material of seven randomly selected CCA samples, followed by rinsing the chiseled surface and surface material with 0.22 µm filtered seawater into a 50 mL sterile conical tube labeled 'Endolith'. The remains of each sample were then crushed with a hammer on a clean, dry surface and the innermost crushed rock placed in 30 mL of 0.22 µm filtered seawater in a 50 mL conical tube labeled 'Endolith'. The CCA samples were split into two Endolith and five Epilith replicate incubations using 20 mL and 10 mL of each sample, respectively. This was done to balance the presumably lower biomass of the endolith sample against the higher biomass epilith. Three of the five epilith replicates were incubated in 1.5 L chambers with lids custom fit for use with a MANTA sensor (only three such incubation chambers were available) while all other incubations were carried out in 1 L chambers (measured by

PreSens optodes). Each chamber was filled with 0.22 µm filtered seawater before inoculation with a respective sample, then sealed with the sensor/lid combo, making sure to eliminate any headspace in the chamber. Incubations ran for 48 hours, allowing two full diurnal cycles to take place.

Estimation of Net Oxygen Production from Time Series Graphs

In order to compare the integrated DO concentration data for both day and night peaks across previously published studies and our own, the area under the curve of time series DO plots was analyzed using ImageJ (https://imagej.nih.gov/ij/). The area under the peak was traced manually for daytime and nighttime, using a baseline running from the points on either side of the curve as it enters and exits the timeframe designated day on the graph (day), or the lowest points on either side of the nighttime peak (night). The area was then calculated in pixels and the pixel area for night divided by the pixel area for day.

References

1. Canfield DE (2013) *Science Essentials : Oxygen : A Four Billion Year History* (Princeton University Press, Princeton, NJ, USA) Available at: http://site.ebrary.com/lib/ucsd/docDetail.action?docID=10801286.
2. Lyons TW, Reinhard CT, Planavsky NJ (2014) The rise of oxygen in Earth's early ocean and atmosphere. *Nature* 506(7488):307–15.
3. Hagemann M, et al. (2016) Evolution of photorespiration from cyanobacteria to land plants, considering protein phylogenies and acquisition of carbon concentrating mechanisms. *J Exp Bot* 67(10):2963–2976.
4. Kramer DM, Avenson TJ, Edwards GE (2004) Dynamic flexibility in the light reactions of photosynthesis governed by both electron and proton transfer reactions. *Trends Plant Sci* 9(7):349–57.
5. Bassham JA, Benson AA, Calvin M (1950) *The Path of Carbon in Photosynthesis VIII. The Role of MalicAcid* (Berkeley, CA) doi:10.2172/910351.
6. Smith S V (1981) Marine macrophytes as a global carbon sink. *Science* 211(4484):838–40.
7. Tappan H (1968) Primary production, isotopes, extinctions and the atmosphere. *Palaeogeogr Palaeoclimatol Palaeoecol* 4(3):187–210.
8. MacIntyre HL, Geider RJ, Miller DC (1996) Microphytobenthos: The Ecological Role of the "Secret Garden" of Unvegetated, Shallow-Water Marine Habitats. I. Distribution, Abundance and Primary Production. *Estuaries* 19(2):186.
9. Ettwig KF, et al. (2010) Nitrite-driven anaerobic methane oxidation by oxygenic bacteria. *Nature* 464(7288):543–548.

10. Schaffner I, et al. (2015) Dimeric chlorite dismutase from the nitrogen-fixing cyanobacterium Cyanothece sp. PCC7425. *Mol Microbiol* 96(5):1053–68.

11. Kinsey D (DW) (1985) Metabolism, calcification and carbon production. I. System level studies. Available at: http://epubs.aims.gov.au//handle/11068/3465 [Accessed November 19, 2015].

12. Odum HT (1957) Primary production measurements in eleven Florida springs and a marine turtle-grass community. *Limnol Oceanogr* 2(2):85–97.

13. Kraines S, Suzuki Y, Yamada K, Komiyama H (1996) Separating Biological and Physical Changes in Dissolved Oxygen Concentration in a Coral Reef. *Limnol Oceanogr* 41(8):1790–1799.

14. Sournia A (1976) Oxygen metabolism of a fringing reef in French polynesia. *Helgoländer Wissenschaftliche Meeresuntersuchungen* 28:401–410.

15. Kraines S, Yanagi T, Isobe M, Komiyama H (1998) Wind-wave driven circulation on the coral reef at Bora Bay, Miyako Island. *Coral Reefs* 17(2):133–143.

16. Viaroli P, Christian RR (2004) Description of trophic status, hyperautotrophy and dystrophy of a coastal lagoon through a potential oxygen production and consumption index—TOSI: Trophic Oxygen Status Index. *Ecol Indic* 3(4):237–250.

17. Krumme U, Herbeck LS, Wang T (2012) Tide- and rainfall-induced variations of physical and chemical parameters in a mangrove-depleted estuary of East Hainan (South China Sea). *Mar Environ Res* 82:28–39.

18. Rheuban JE, Berg P, McGlathery KJ (2014) Multiple timescale processes drive ecosystem metabolism in eelgrass (Zostera marina) meadows. *Mar Ecol Prog Ser* 507:1–13.

19. Reimers CE, et al. (2012) Benthic oxygen consumption rates during hypoxic conditions on the Oregon continental shelf: Evaluation of the eddy correlation method. *J Geophys Res* 117(C2):C02021.

20. Campion-Alsumard T, Romano JC, Peyrot-Clausade M, Campion J, Paul R (1993) Influence of some coral reef communities on the calcium carbonate budget of Tiahura reef (Moorea, French Polynesia). *Mar Biol* 115(4):685–693.

21. Kayanne H, et al. (2008) Integrated monitoring system for coral reef water pCO2, carbonate system and physical parameters. *Proc Ninth Int Coral Reef Symp, Bali* 2(October):1079–1084.

22. Luz B, Barkan E (2009) Net and gross oxygen production from O2/Ar, 17O/ 16O and 18O/16O ratios. *Aquat Microb Ecol* 56(2–3):133–145.

23. Haas AF, et al. (2013) Influence of coral and algal exudates on microbially mediated reef metabolism. *PeerJ* 1:e108.

24. Takeshita Y, et al. (2016) Assessment of net community production and calcification of a coral reef using a boundary layer approach. *J Geophys Res Ocean*. doi:10.1002/2016JC011886.

25. Barnett L, Seth AK (2014) The MVGC multivariate Granger causality toolbox: a new approach to Granger-causal inference. *J Neurosci Methods* 223:50–68.

26. Hench JL, Leichter JJ, Monismith SG (2008) Episodic circulation and exchange in a wave-driven coral reef and lagoon system. *Limnol Oceanogr* 53(6):2681–2694.

27. Nelson CE, Alldredge AL, McCliment EA, Amaral-Zettler LA, Carlson CA (2011) Depleted dissolved organic carbon and distinct bacterial communities in the water column of a rapid-flushing coral reef ecosystem. *ISME J* 5(8):1374–1387.

28. Leichter JJ, et al. (2013) Biological and physical interactions on a tropical island coral reef transport and retention processes on Moorea, French Polynesia.

29. Gan F, Bryant DA (2015) Adaptive and acclimative responses of cyanobacteria to far-red light. *Environ Microbiol*. doi:10.1111/1462-2920.12992.

30. Sharma P, Jha AB, Dubey RS, Pessarakli M (2012) Reactive Oxygen Species, Oxidative Damage, and Antioxidative Defense Mechanism in Plants under Stressful Conditions. *J Bot* 2012:1–26.

31. Jackson J, Donovan M, Cramer K, Lam V (2014) Status and trends of Caribbean coral reefs: 1970-2012.

32. Collins JR, Raymond P a., Bohlen WF, Howard-Strobel MM (2013) Estimates of New and Total Productivity in Central Long Island Sound from In Situ Measurements of Nitrate and Dissolved Oxygen. *Estuaries and Coasts* 36:74–97.

33. Baumann H, Wallace RB, Tagliaferri T, Gobler CJ (2014) Large Natural pH, CO2 and O2 Fluctuations in a Temperate Tidal Salt Marsh on Diel, Seasonal, and Interannual Time Scales. *Estuaries and Coasts*:220–231.

34. Shen J, Wang T, Herman J, Mason P, Arnold GL (2008) Hypoxia in a Coastal Embayment of the Chesapeake Bay: A Model Diagnostic Study of Oxygen Dynamics. *Estuaries and Coasts* 31(4):652–663.

35. Wild C, Niggl W, Naumann MS, Haas AF (2010) Organic matter release by Red Sea coral reef organisms-Potential effects on microbial activity and in situ O2 availability. *Mar Ecol Prog Ser* 411:61–71.

36. Long MH, Berg P, de Beer D, Zieman JC (2013) In situ coral reef oxygen metabolism: an eddy correlation study. *PLoS One* 8(3):e58581.

37. Yates KK, Dufore C, Smiley N, Jackson C, Halley RB (2007) Diurnal variation of oxygen and carbonate system parameters in Tampa Bay and Florida Bay. *Mar Chem* 104(1–2):110–124.

38. Martinez JA, Smith CM, Richmond RH (2012) Invasive algal mats degrade coral reef physical habitat quality. *Estuar Coast Shelf Sci* 99:42–49.

39. McGillis WR, Langdon C, Loose B, Yates KK, Corredor J (2011) Productivity of a coral reef using boundary layer and enclosure methods. *Geophys Res Lett* 38(3):2–6.

40. Frankignoulle M, et al. (1996) Carbon fluxes in coral reef. II. Eulerian study of inorganic carbon dynamic and measurement of air-sea exchange. *Mar Ecol Prog Ser* 145:123–132.

41. Santos IR, Glud RN, Maher D, Erler D, Eyre BD (2011) Diel coral reef acidification driven by porewater advection in permeable carbonate sands, Heron Island, Great Barrier Reef. *Geophys Res Lett* 38(3):1–5.

42. Yamamoto S, Kayanne H, Tokoro T, Kuwae T, Watanabe A (2015) Total alkalinity flux in coral reefs estimated from eddy covariance and sediment pore-water profiles. *Limnol Oceanogr* 60:229–241.

43. LaRiviere D., Autenrieth R.L., Bonner J.S. (2004) Redox dynamics of a tidally-influenced wetland on the San Jacinto River. *Estuaries* 27(2):253–264.

44. Tobias CR, Böhlke JK, Harvey JW (2007) The oxygen-18 isotope approach for measuring aquatic metabolism in high productivity waters. *Limnol Oceanogr* 52(4):1439–1453.

45. Howarth RW, et al. (2014) Metabolism of a nitrogen-enriched coastal marine lagoon during the

PeerJ Preprints NOT PEER-REVIEWED

summertime. *Biogeochemistry* 118(1–3):1–20.

46. Hanson PC, Bade DL, Carpenter SR, Kratz TK (2003) Lake metabolism: Relationships with dissolved organic carbon and phosphorus. *Limnol Oceanogr* 48(3):1112–1119.

PeerJ Preprints NOT PEER-REVIEWED

Figure 1. Nighttime spikes in dissolved oxygen concentrations are global phenomena.

Each number corresponds to a dataset identified during a literature search (blue dots and numbers) or a dataset presented in this study (orange dots and numbers) consisting of dissolved oxygen concentration measurements across day and night times for at least 24 hours. The equator, tropics, and polar latitudes are labeled.

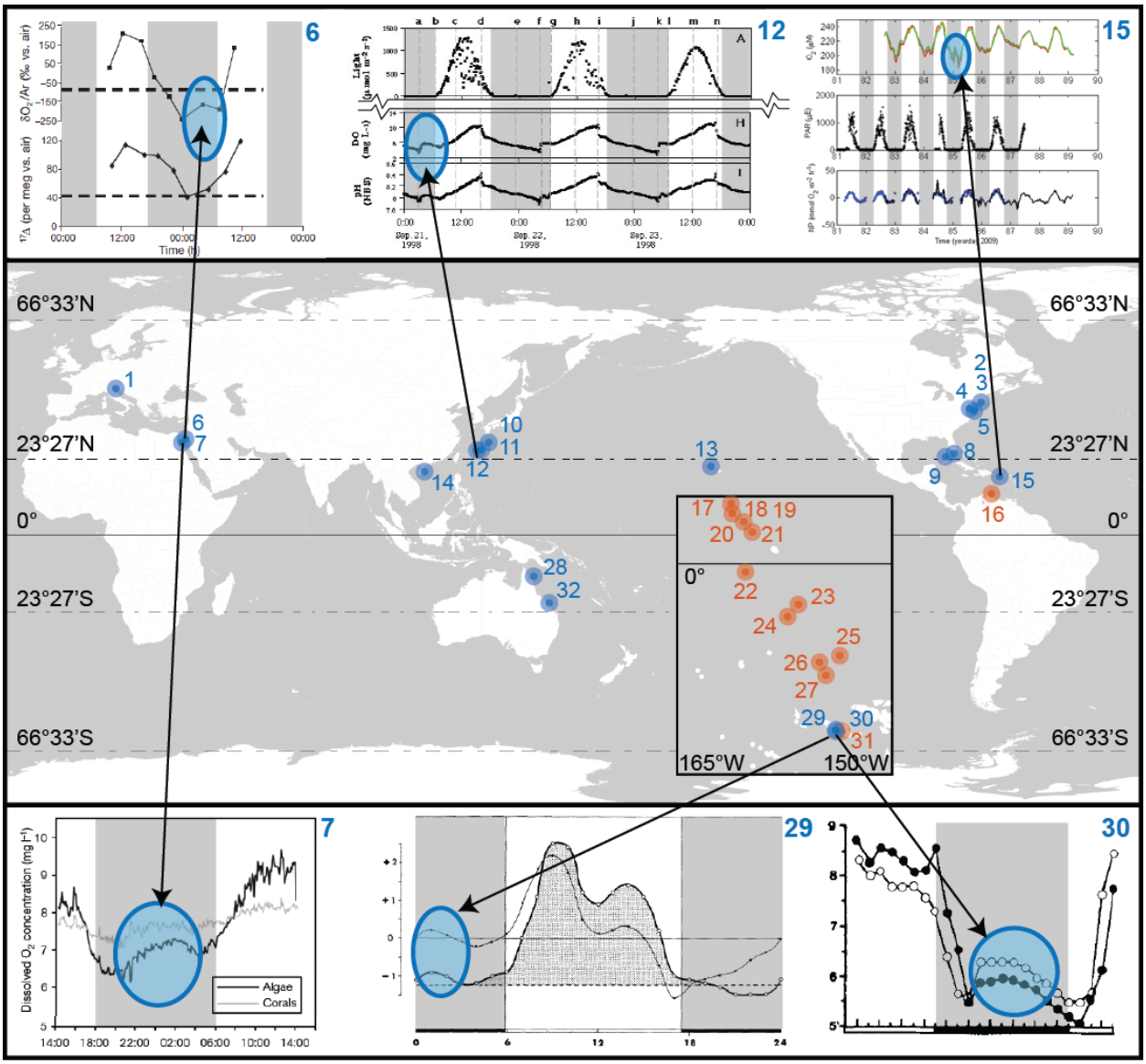

Figure 2. Nighttime spikes in dissolved oxygen concentration often align with temperature spikes in turbulent environments.

The number of nighttime DO spikes for each of our datasets presented in this study were compared to simultaneous temperature measurements as a proxy for shifting thermoclines. Overall, 37% of the nighttime DO spikes show concurrent temperature spikes, with nearly all concurrent spikes occurring at turbulent fore reef sites in the Line Islands (Kingman through Flint). However, changes in current do not always occur alongside shifts in temperature, so this data may under-represent the actual influence of current shifts on DO concentration. Palmyra data are combined from both the 2010 and 2014 studies. All other data represent single deployments spanning one month or less.

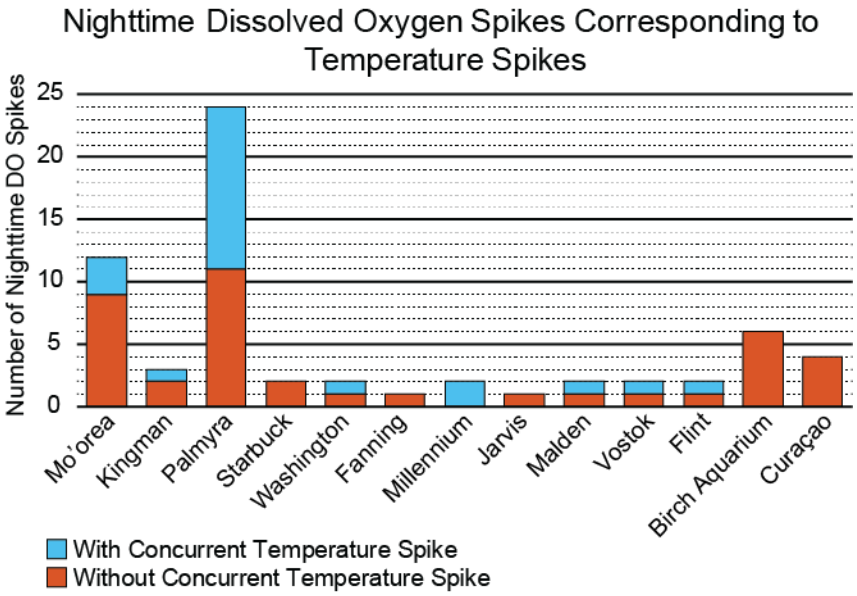

Figure 3. Nighttime spikes in dissolved oxygen concentrations occur repeatedly across different islands on different dates with and without any predictive physical variable.

High resolution autonomous logging of dissolved oxygen for A.) Mo'orea over Sept. 5-8, 2011, without a predictive physical variable; B.) Mo'orea over Sept. 1-3 2011, where wind was found to be a predictor of dissolved oxygen concentration; C.) Starbuck Island over Oct. 26-29, 2013, without a predictive physical variable; D.) Millennium Island over Nov. 5-8, 2013 where moon phase (new moon) was found to be a predictor of dissolved oxygen concentration. cBITs were used in all panels, except where the vertical dotted line on panels C and D indicates removal of the cBIT. Grey areas indicate night times. Horizontal dashed lines and solid bars on the y-axis highlight the amplitude of select DO spikes for those sensors/sites.

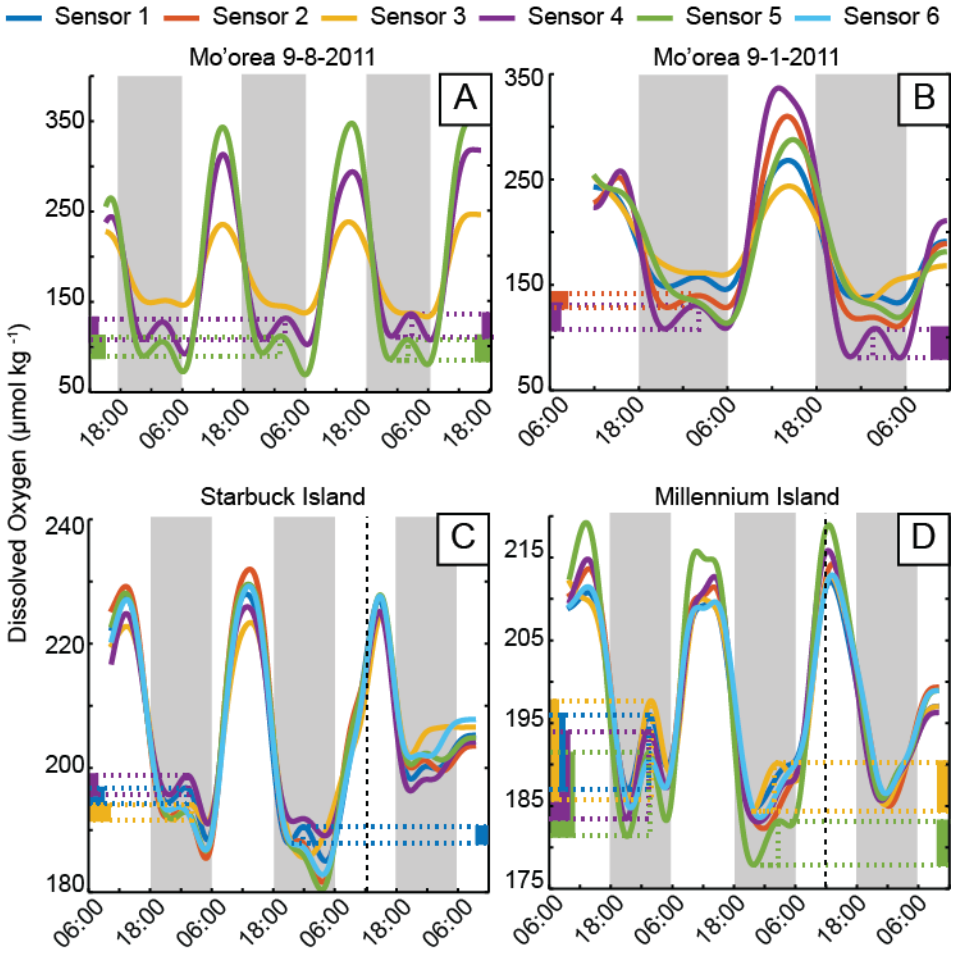

PeerJ Preprints NOT PEER-REVIEWED

Figure 4. Nighttime DO spikes can be seen over longer periods in highly variable oceanographic contexts.

High resolution autonomous logging of dissolved oxygen concentration for A) Palmyra Atoll, Central Pacific, September 8-24, 2014; B) Curacao, Southern Caribbean, May 7-13, 2015; C.) Birch Aquarium coral tanks, San Diego, CA, USA, Aug 8-12, 2014. Grey areas indicate night (or zero PAR) times. Horizontal dashed lines and solid bars on the y-axis highlight the amplitude of select DO spikes for those sensors/sites.

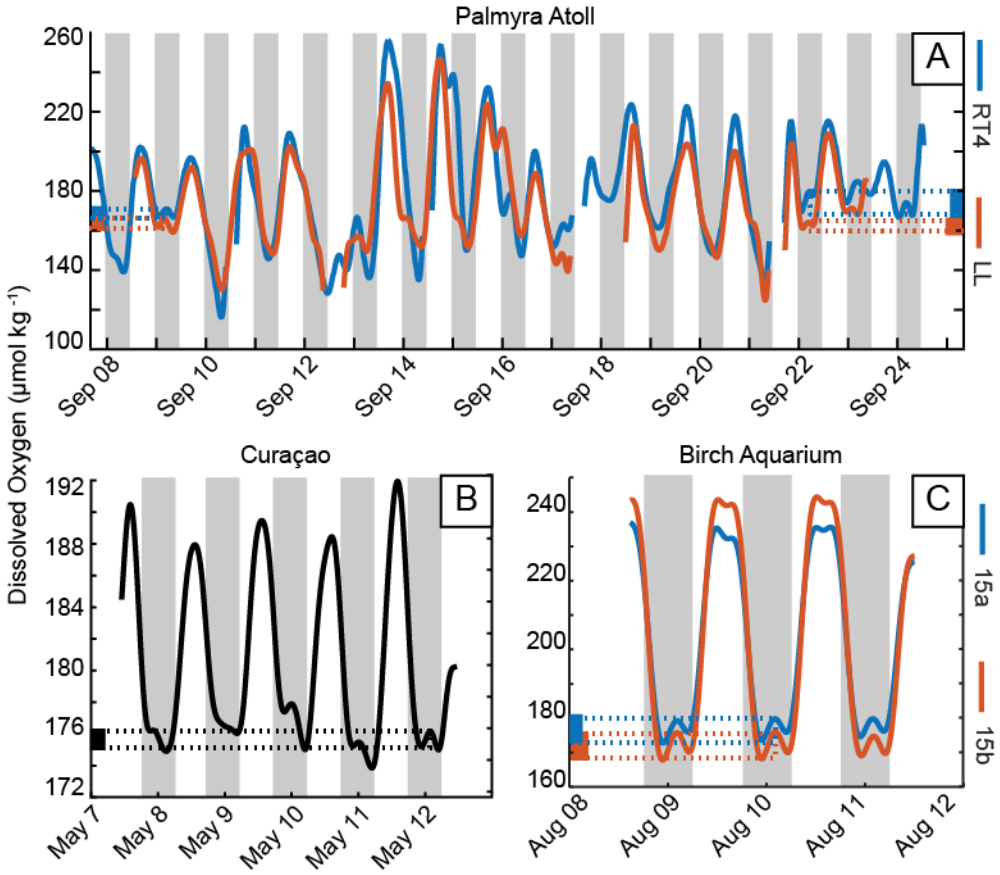

PeerJ Preprints NOT PEER-REVIEWED

Figure 5. Laboratory incubations show that the DO spike can be recreated in a controlled setting using biological samples.

A) 12-hour dark incubations of intact CCA samples at the CARMABI facility during 2015. These CCA samples were normalized to a seawater displacement volume of 500 mL and incubated in partially sealed 2 L cylindrical chambers in a light and temperature controlled environment (see Supplemental Methods). B) 48-hour simulated diurnal incubation of the surface community of mechanically fractionated (via hammer and chisel) CCA rhodoliths at the CARMABI facility during 2016. 10 mL of crushed slurry consisting of the top 1 mm or so of several rhodoliths was added to 1 L of sterile seawater and placed in a fully sealed 1 L cylindrical chamber in a light and temperature controlled environment (see Supplemental Methods).

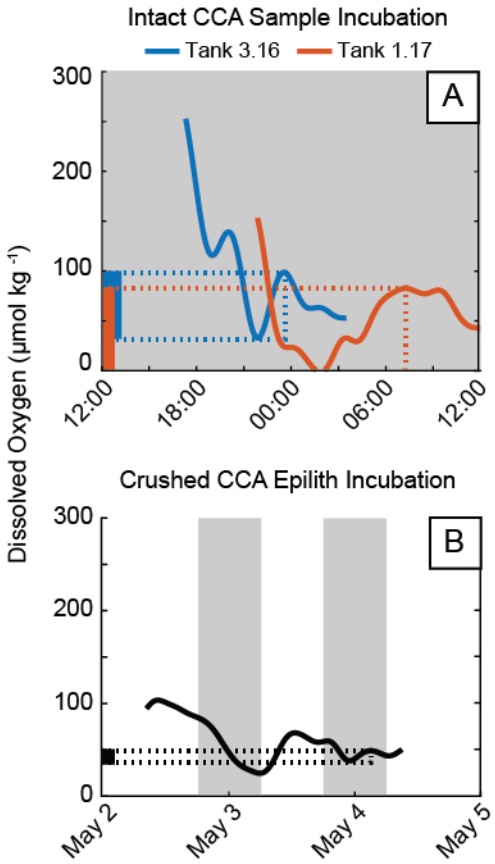

Figure 6. Estimated oxygen input lost due to omission of the nighttime DO spikes from ecosystem oxygen budgets.

Each pie chart represents the total integrated nighttime DO spikes for each time series data set presented here (orange slice) divided by the daily integrated DO for that data set. Estimates were made using ImageJ to measure the area under each spike (see Methods for details).

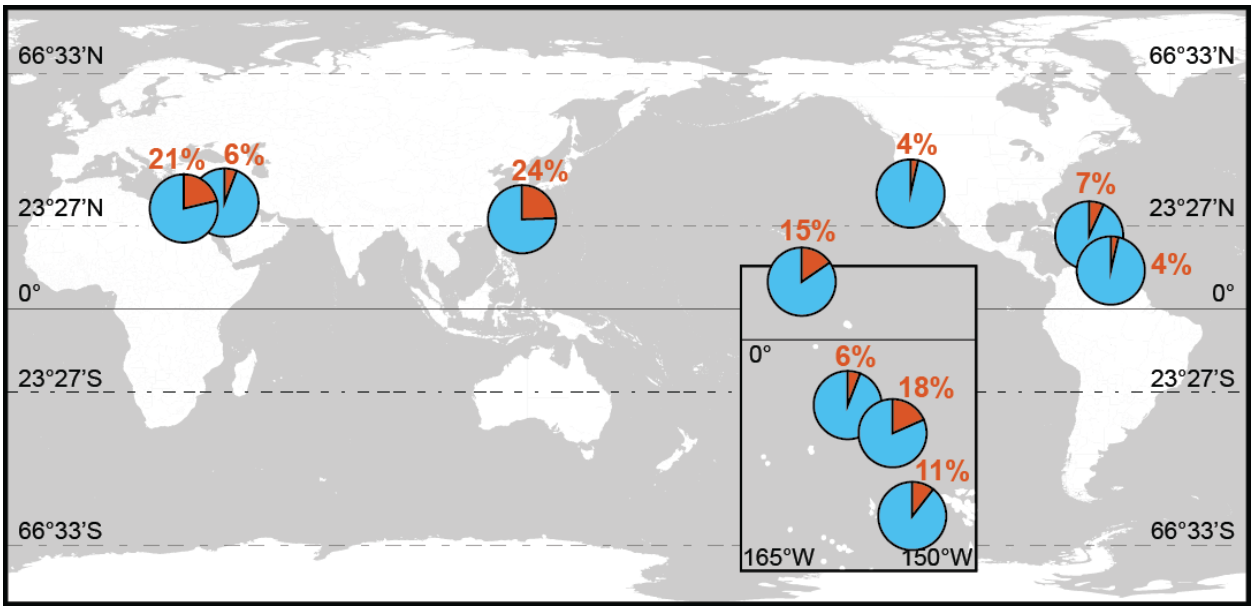

636

PeerJ Preprints NOT PEER-REVIEWED

637 **Supplemental Information**

Figures

Figure S1. Collapsible benthic isolation tent (cBIT) setup used for the 2013 Line Islands and 2011 Mo'orea deployments. Described previously in Haas et al. (2013).

i. Transparent plastic window (polycarbonate)
ii. MANTA multisensor sonde
iii. Steel anchor rings
iv. PVC fabric skirt weighted to diminish flow into and out of cBIT.

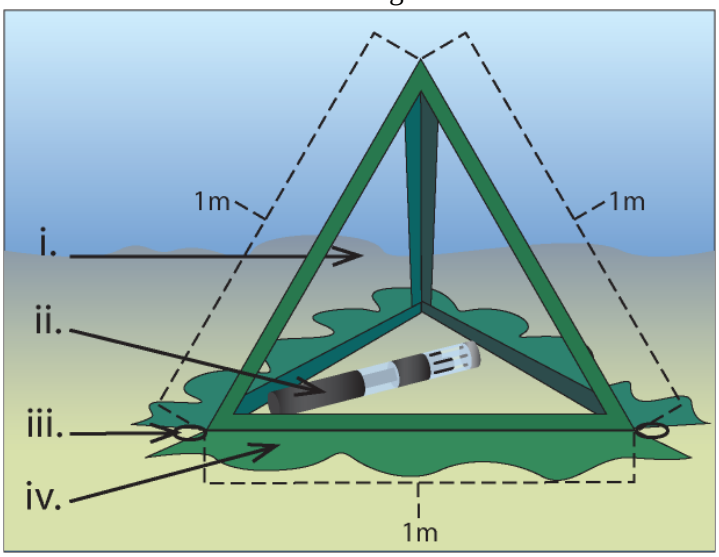

638

PeerJ Preprints NOT PEER-REVIEWED

639 Figure S2. Nighttime spikes in dissolved oxygen (DO) occur in each of the datasets presented in this
640 study.

641 Palmyra data are combined from both the 2013 and 2014 studies. All other data represent deployments
642 spanning one month or less.

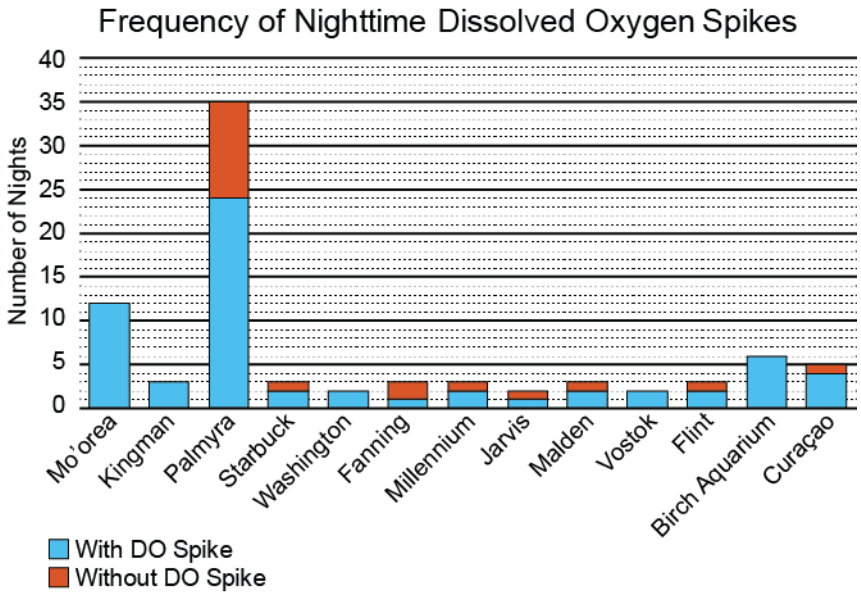

643

644

PeerJ Preprints NOT PEER-REVIEWED

645 Figure S3. DO to temperature comparison data corresponding to Figure 2.

646 Orange triangles indicate a lack of concurrent temperature spike. Data for Palmyra was combined across
647 2013 and 2014 studies in Figure 2.

PeerJ Preprints NOT PEER-REVIEWED

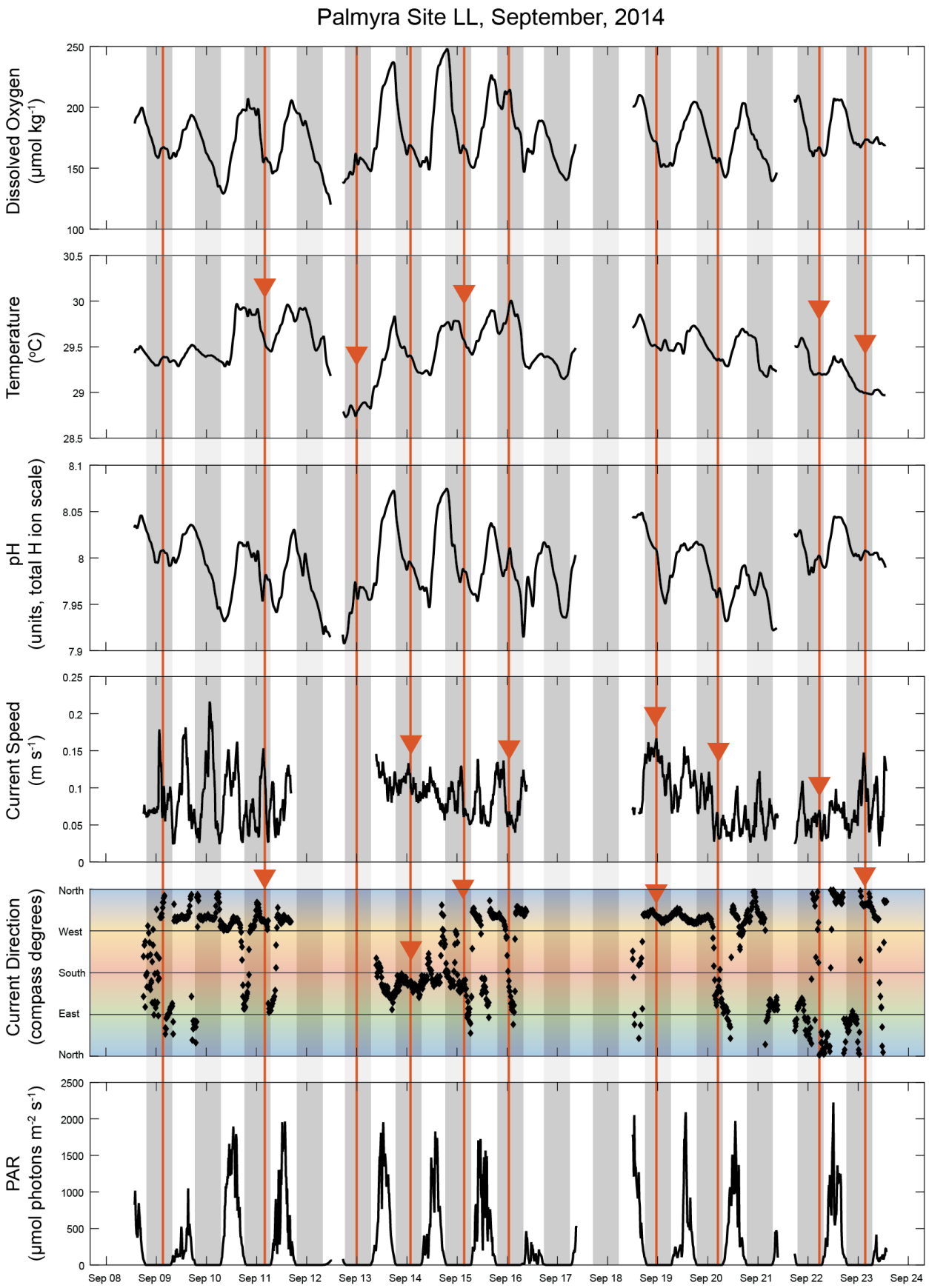

PeerJ Preprints | https://doi.org/10.7287/peerj.preprints.2935v2 | CC BY 4.0 Open Access | rec: 23 May 2017, publ: 23 May 2017

PeerJ Preprints NOT PEER-REVIEWED

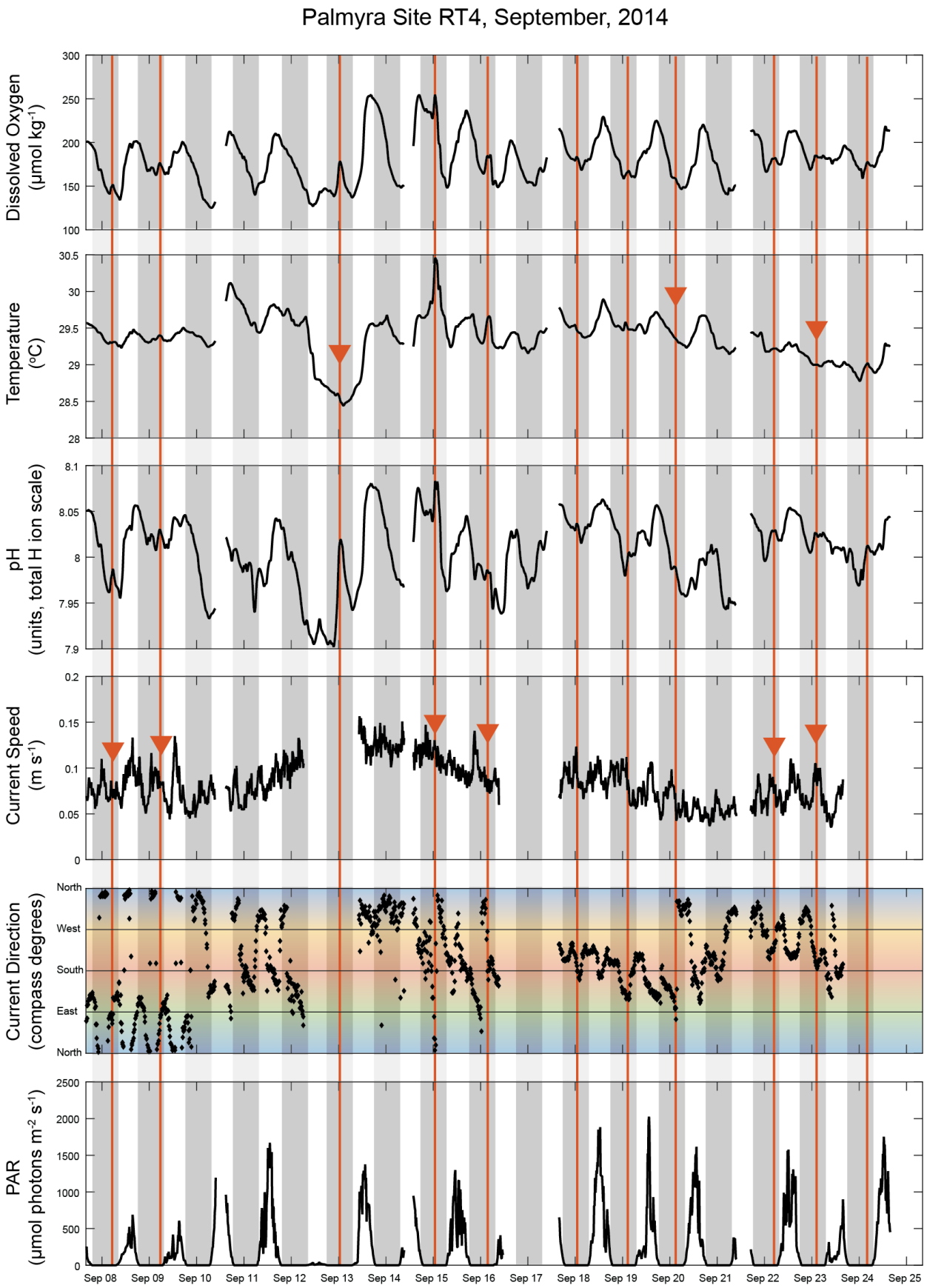

649

PeerJ Preprints NOT PEER-REVIEWED

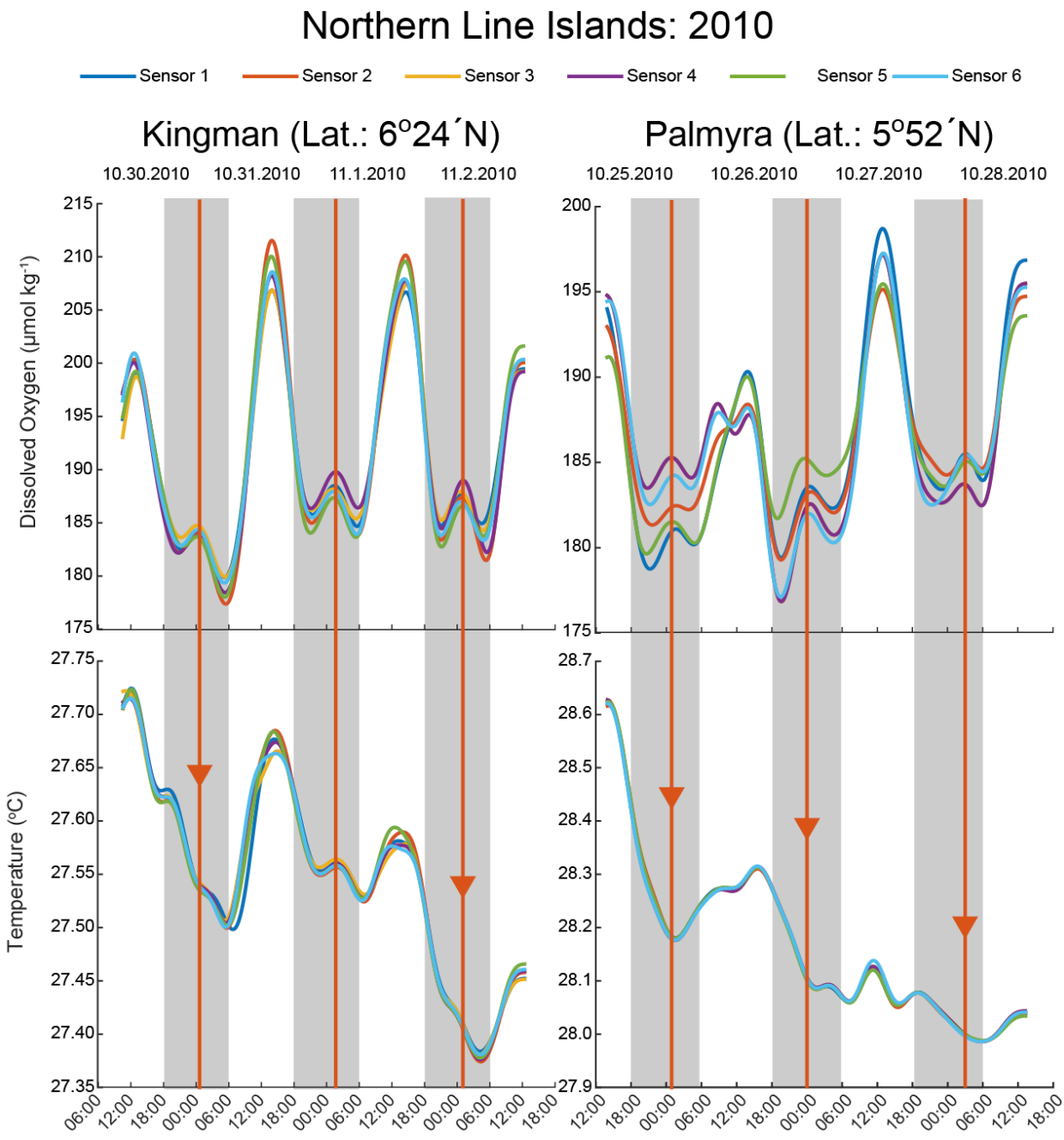

650

651

PeerJ Preprints NOT PEER-REVIEWED

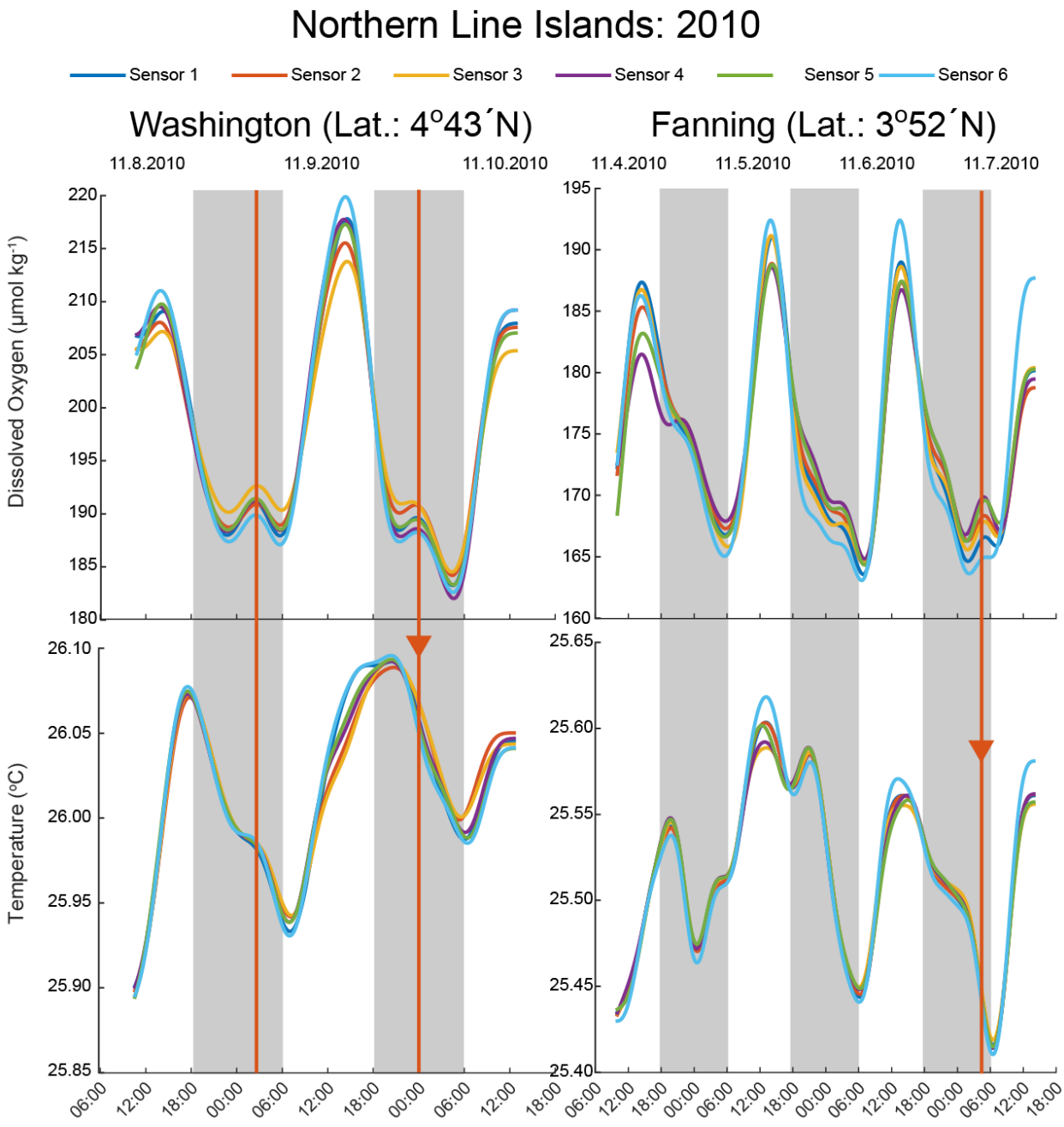

652

653

PeerJ Preprints NOT PEER-REVIEWED

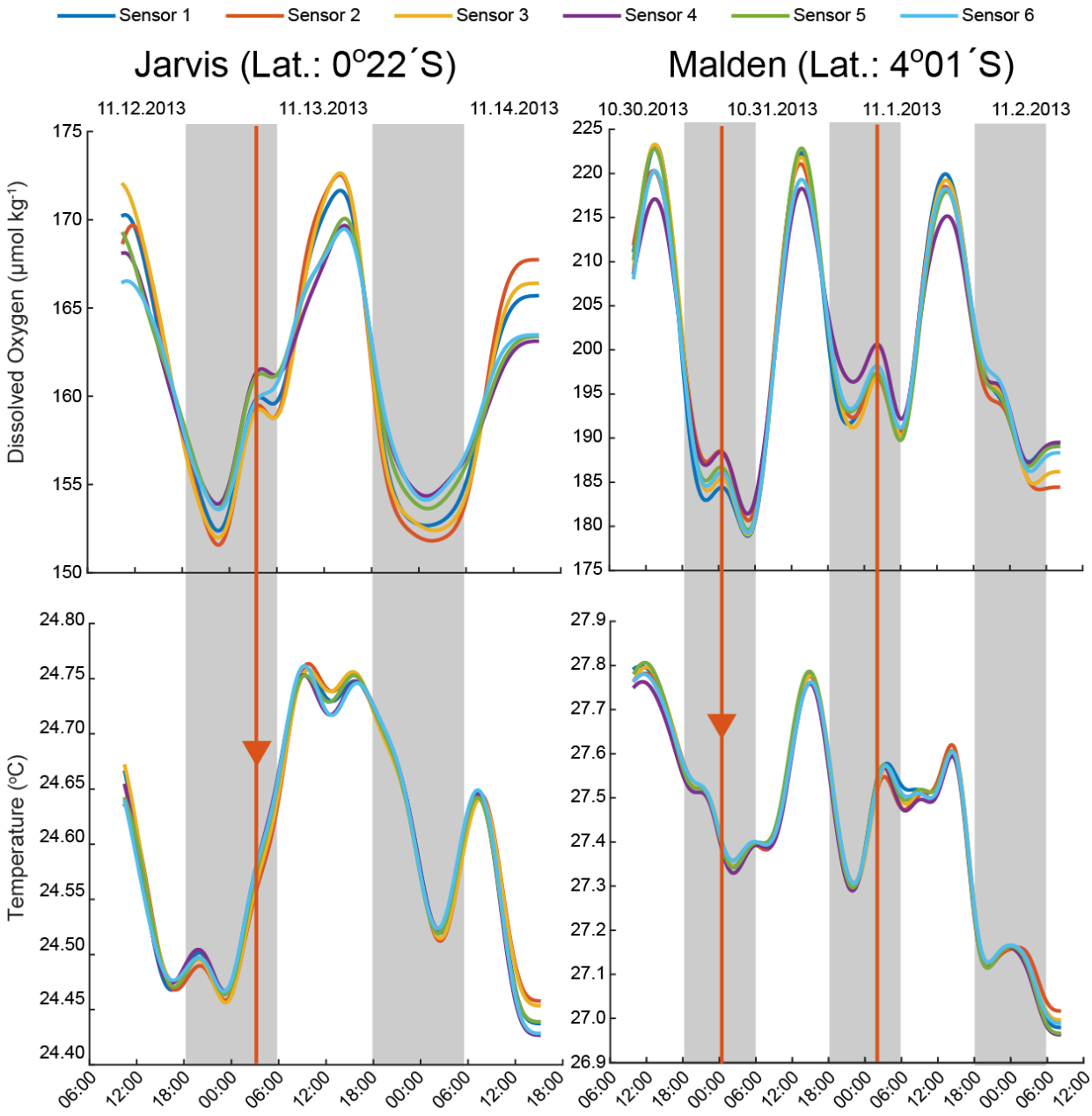

654

655

PeerJ Preprints NOT PEER-REVIEWED

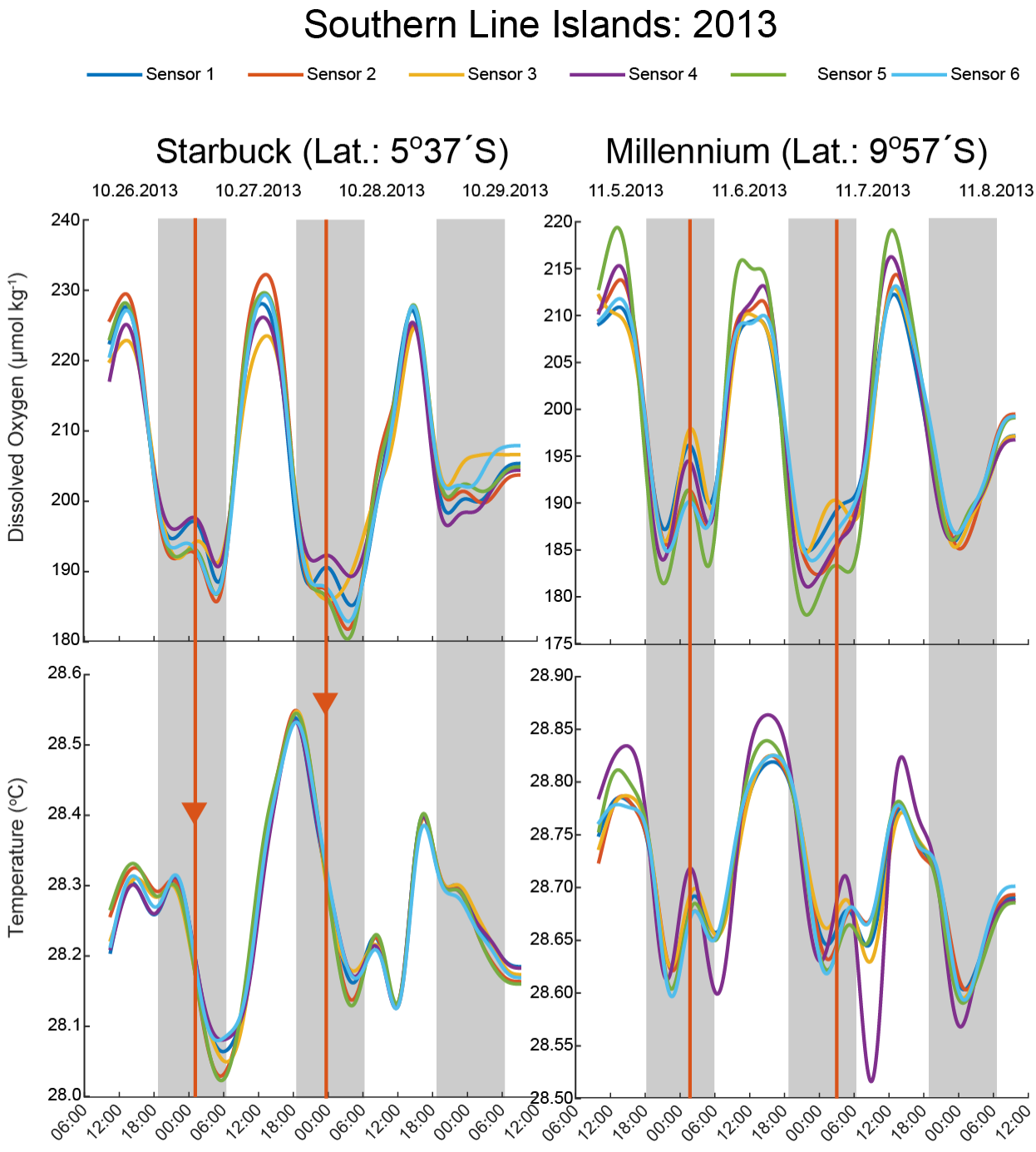

656

657

PeerJ Preprints NOT PEER-REVIEWED

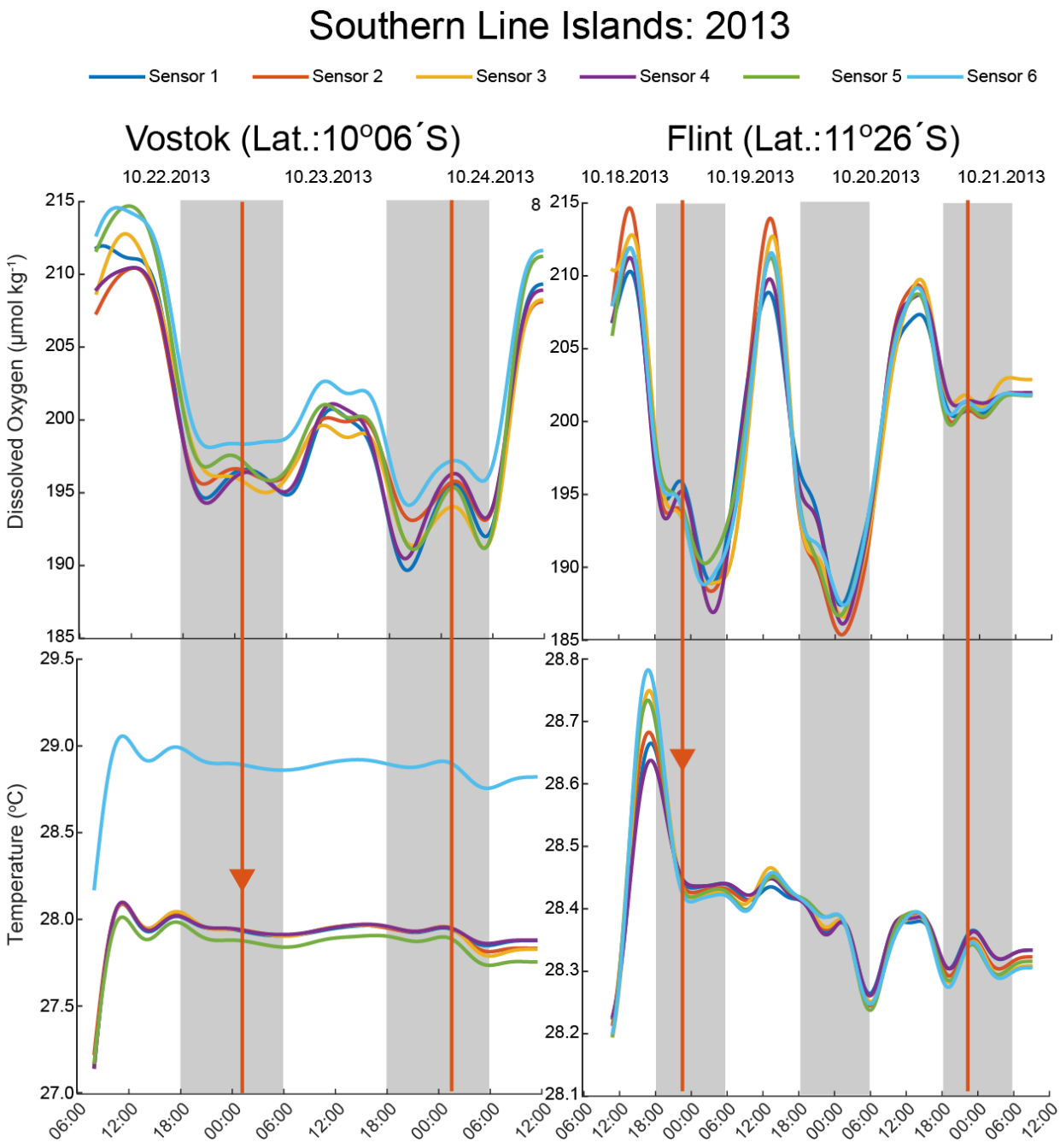

658

659

PeerJ Preprints NOT PEER-REVIEWED

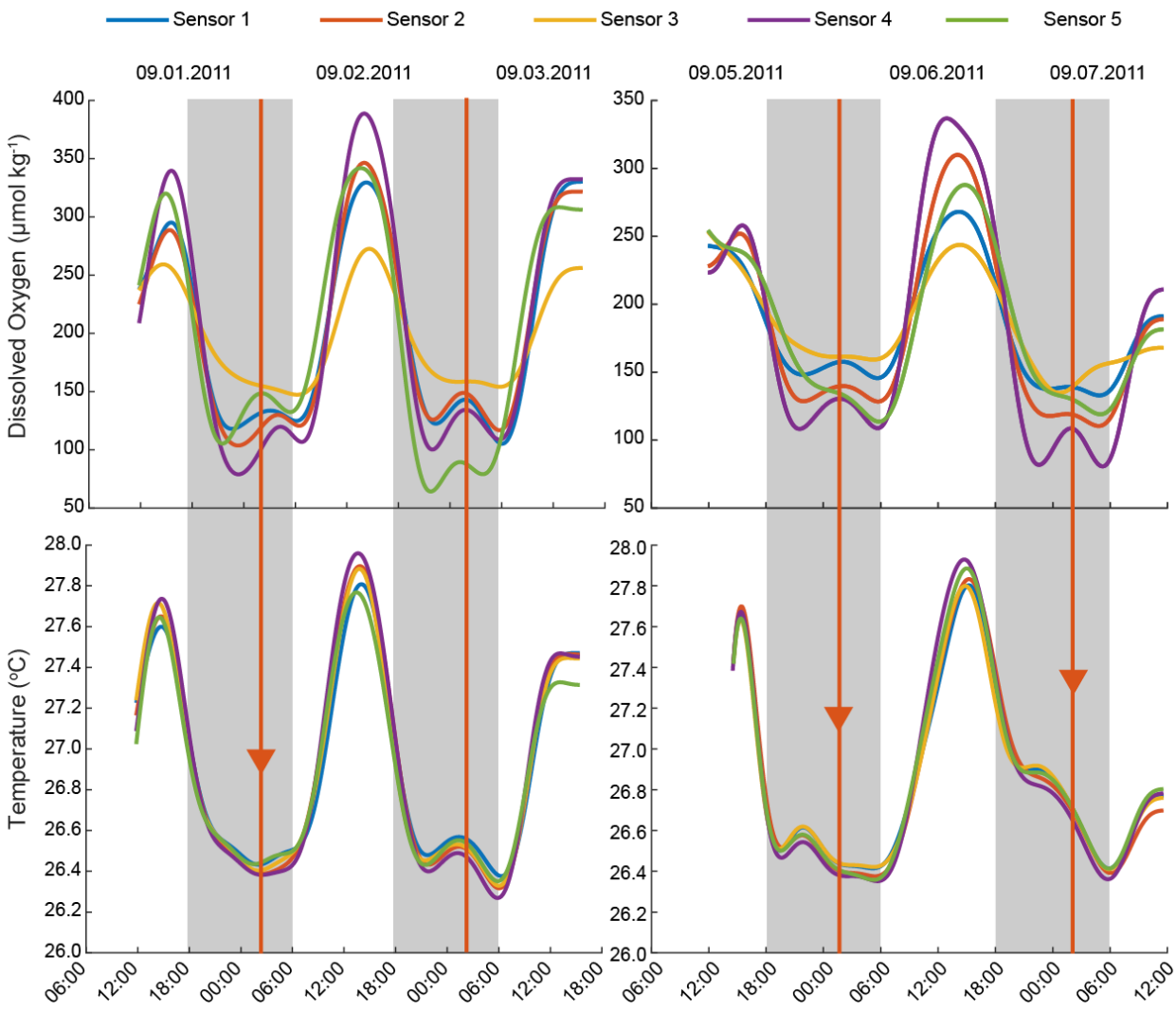

660

661

PeerJ Preprints NOT PEER-REVIEWED

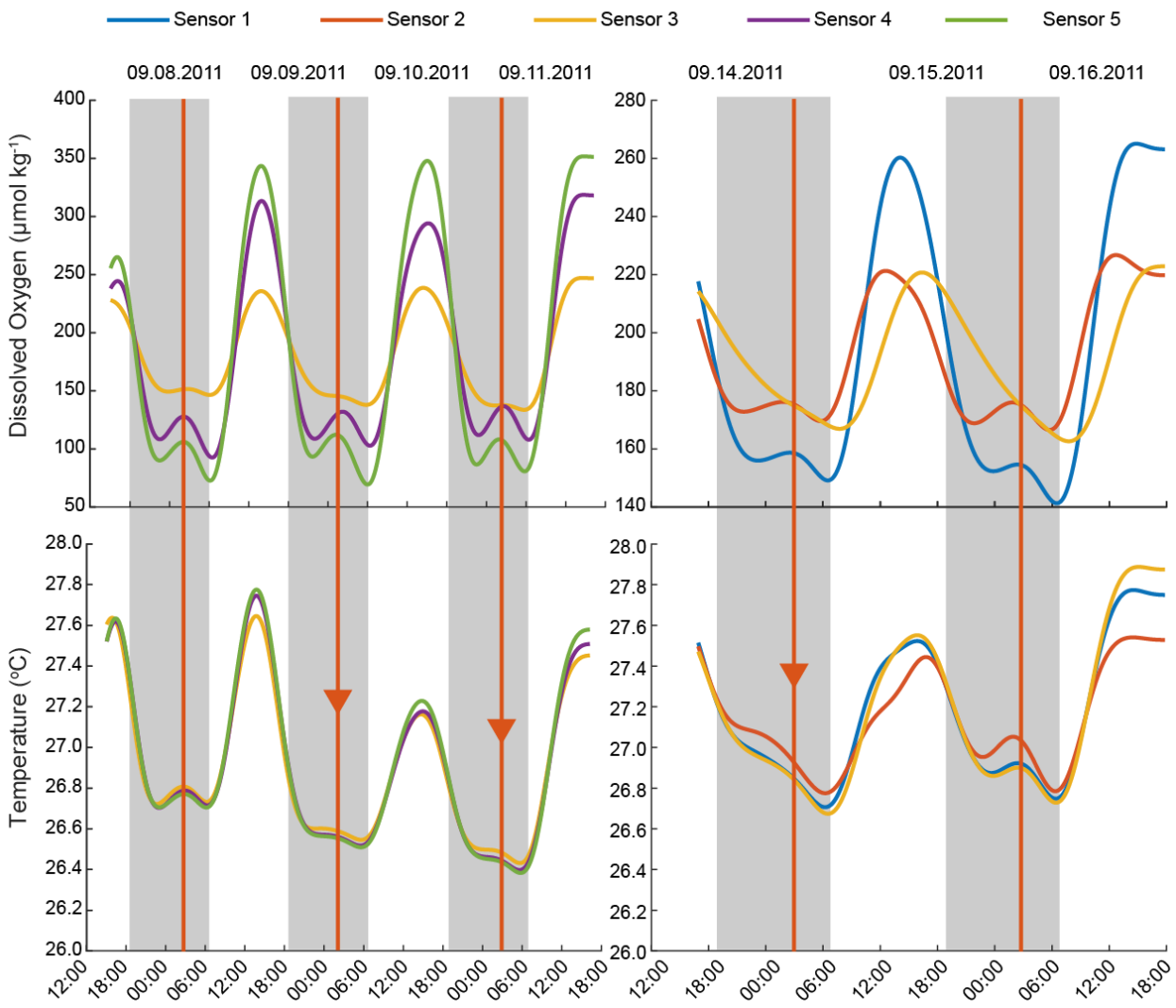

662

663

PeerJ Preprints NOT PEER-REVIEWED

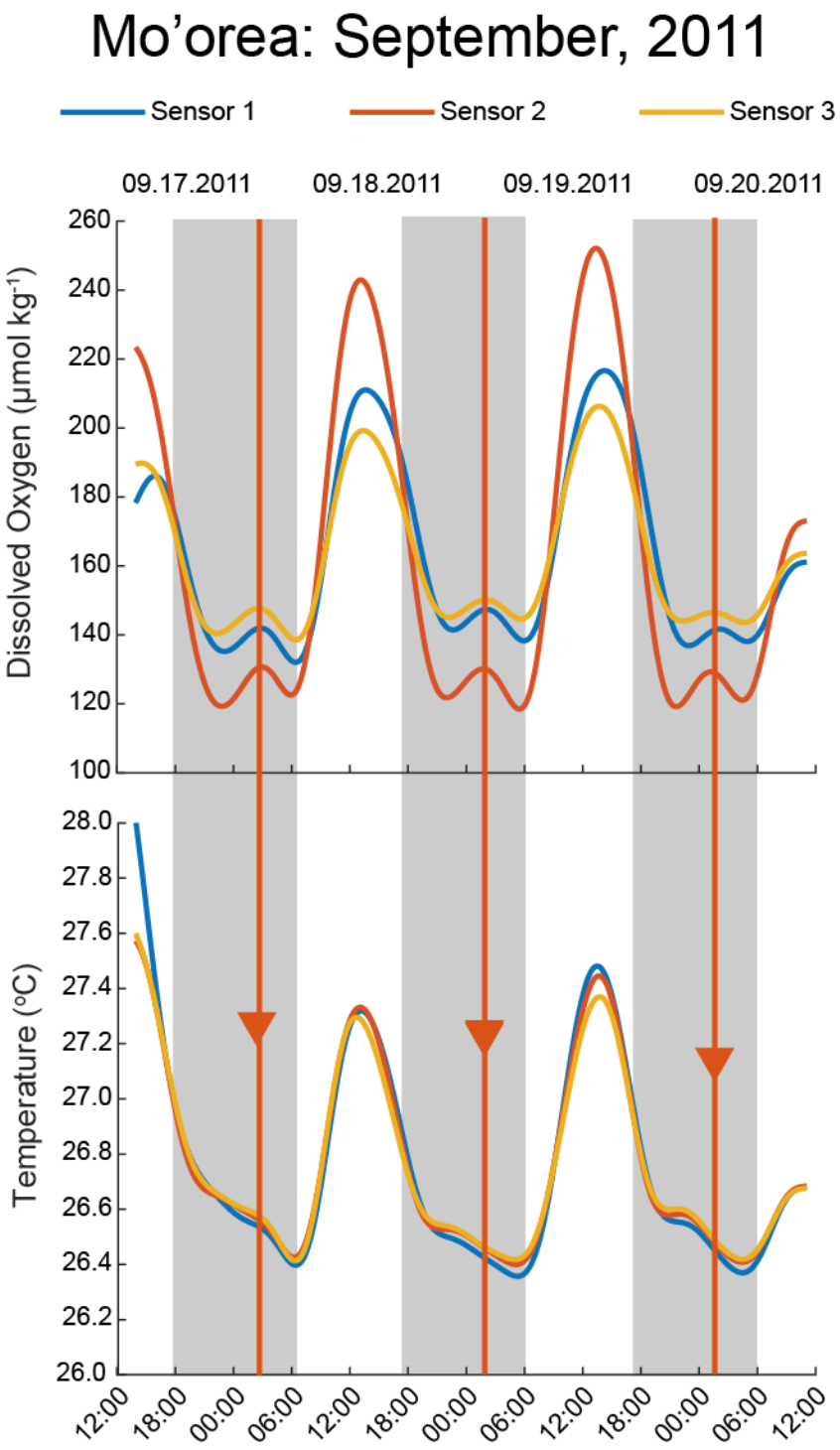

664

665

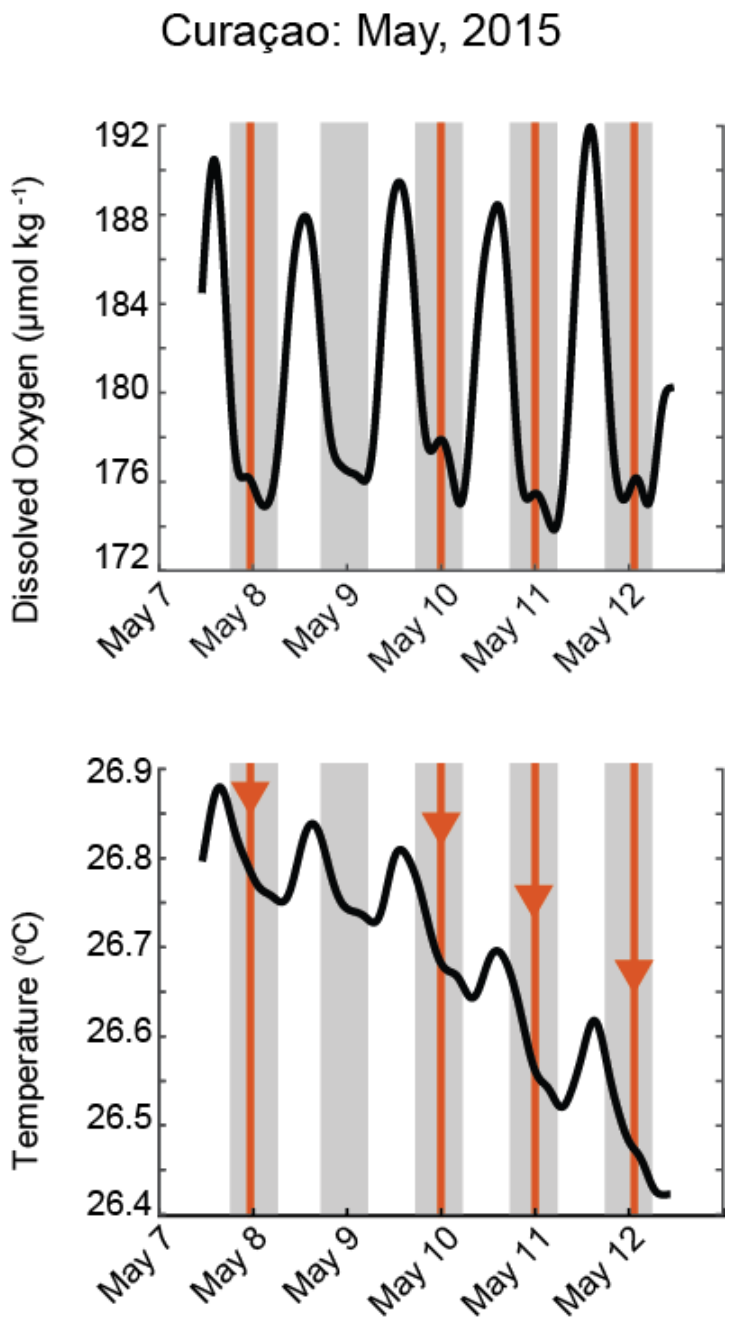
Curaçao: May, 2015
Dissolved Oxygen (µmol kg -1)
192
188
184
180
176
172
May 7
May 8
May 9
May 10
May 11
May 12
Temperature (°C)
26.9
26.8
26.7
26.6
26.5
26.4
May 7
May 8
May 9
May 10
May 11
May 12

666

667

PeerJ Preprints NOT PEER-REVIEWED

Birch Aquarium: August, 2014

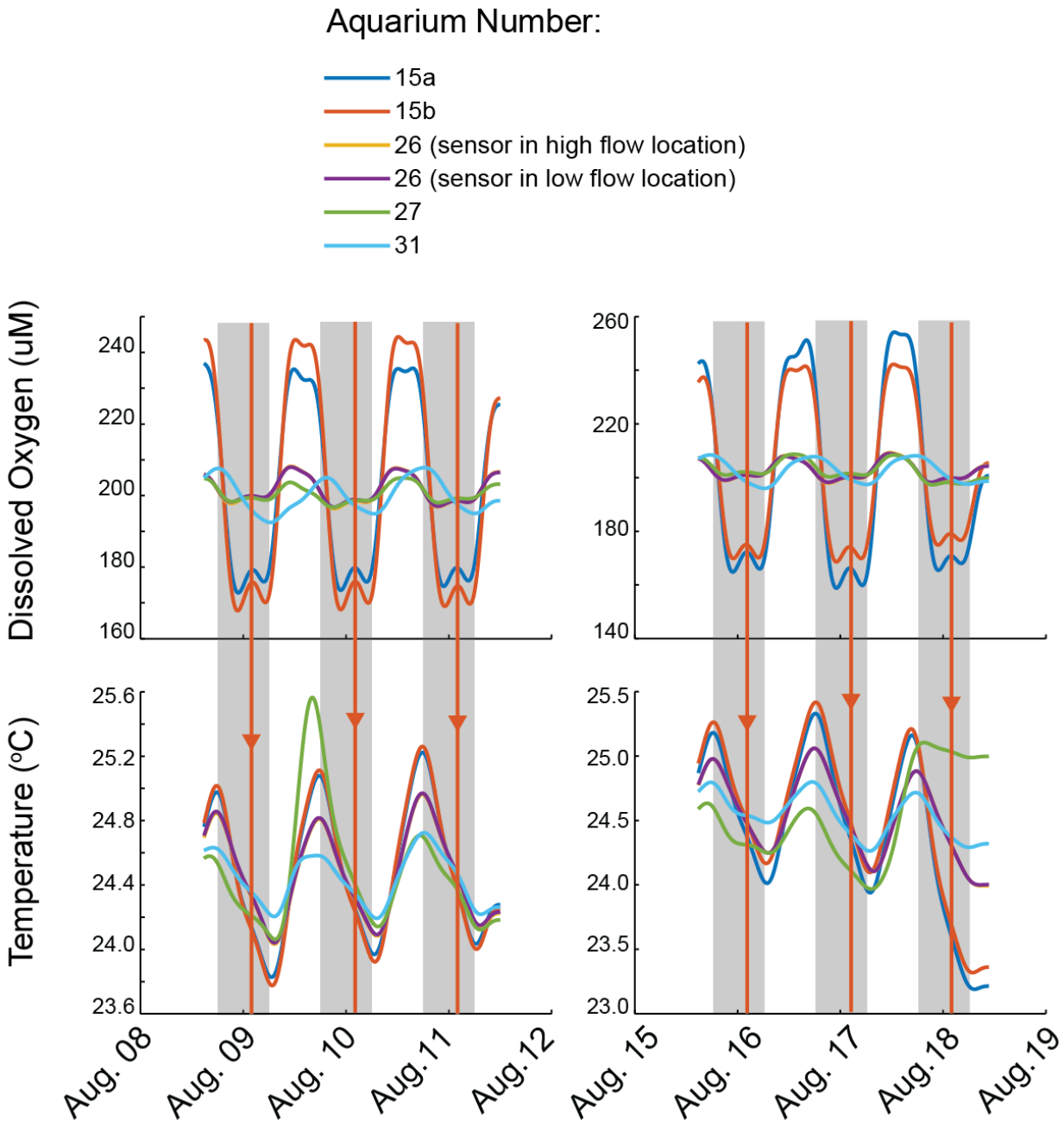

PeerJ Preprints | https://doi.org/10.7287/peerj.preprints.2935v2 | CC BY 4.0 Open Access | rec: 23 May 2017, publ: 23 May 2017

PeerJ Preprints NOT PEER-REVIEWED

Figure S4. Block diagram of laboratory incubation setup used in Curacao.

i. Light-blocking fabric tent over PVC frame
ii. Aquarium lights controlled by a digital timer
iii. MANTA fitted into sealed 1.5 L inucbation chamber
iv. Fiber optic optode fitted into sealed 1 L incubation chamber
v. Temperature controlled water bath
vi. Location of intact samples

Note that the setup used between 2015 and 2016 was very similar, except during 2015 all incubation chambers were 2 L, incubations were only partially sealed, and no light was present.

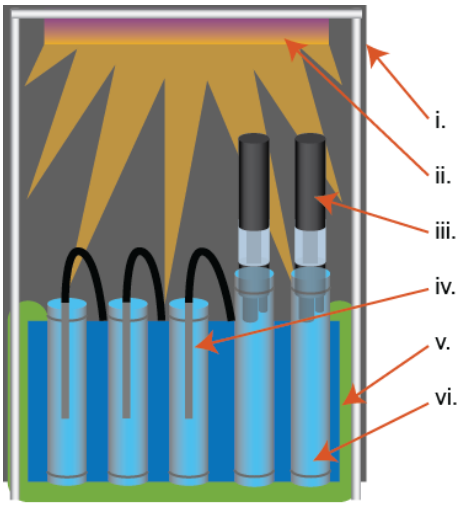

668

PeerJ Preprints NOT PEER-REVIEWED

669 Figure S5. Laboratory Incubations. See Table S4 and Methods for desciptions of sample types and
670 experimental parameters.

A. Incubation Controls (Water Column at 9m – Tank 3.4, Surface Water – 3.14, Dry Rubble – 5.13, Tap water – Tank 4.4)
B. CCA: Tanks 3.16, 1.17, 2.17, 3.18, 4.18
C. Turf: Tanks 3.7, 4.8, 1.10, 1.12, 2.12, 1.13
D. Sediment: Tanks 12, 1.6, 1.11, 2.11, 3.11, 4.11
E. Rubble: Tanks 5.12, 1.14, 2.14, 4.14, 3.15, 4.15
F. Mixed: Tanks 1.7, 2.7, 2.8, 3.8, 1.9, 2.9

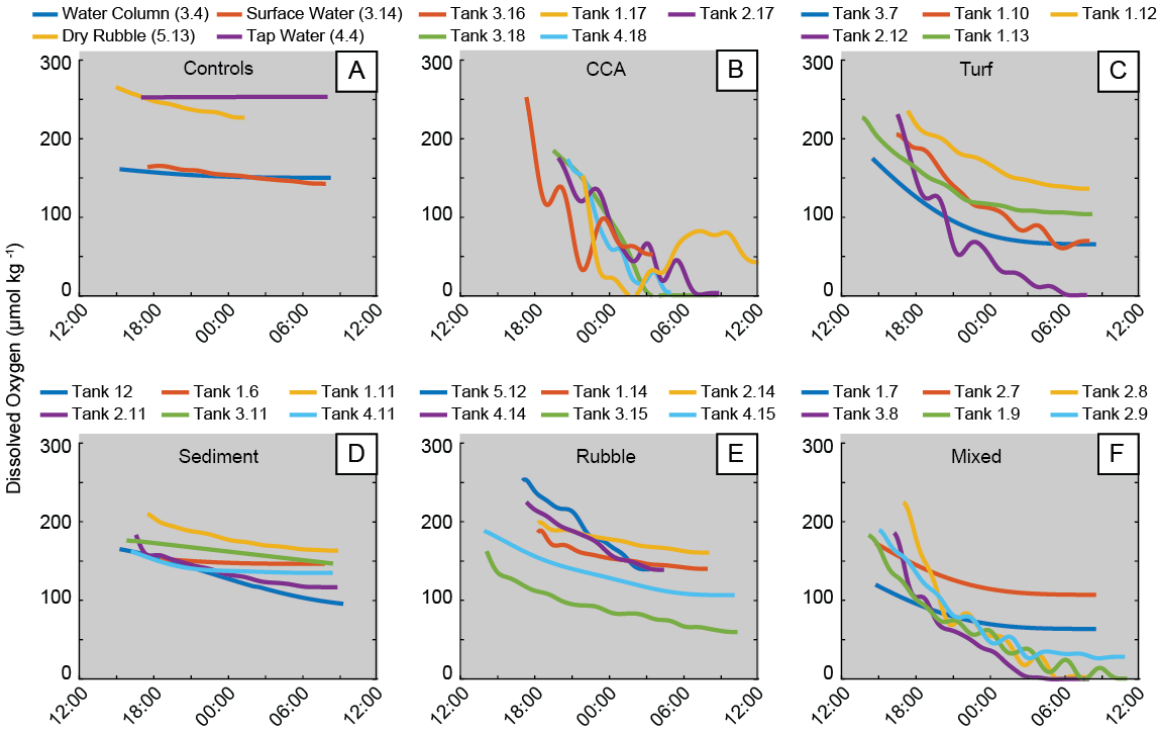

PeerJ Preprints NOT PEER-REVIEWED

Figure S6. Fully enclosed laboratory incubations with fractionation.

See Methods for desciptions of sample types and experimental parameters.

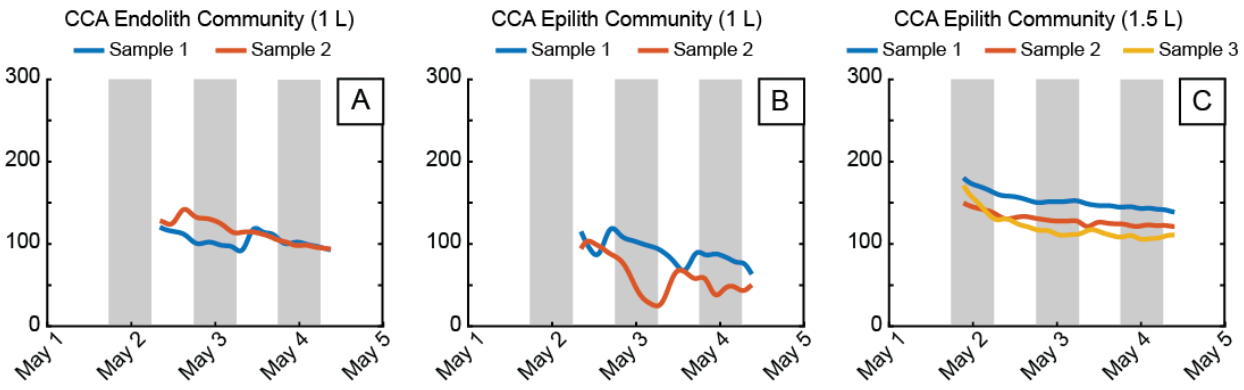

PeerJ Preprints NOT PEER-REVIEWED

Figure S7. CCA Samples taken from Curaçao and Birch Aquarium and housed in aquaria at San Diego State University.

671 CCA samples from Curacao after one week of acclimation at San Diego State University (A.), and (B.)
672 CCA samples from both Birch Aquarium and Curacao after long term establishement in an experimental
673 aquarium.

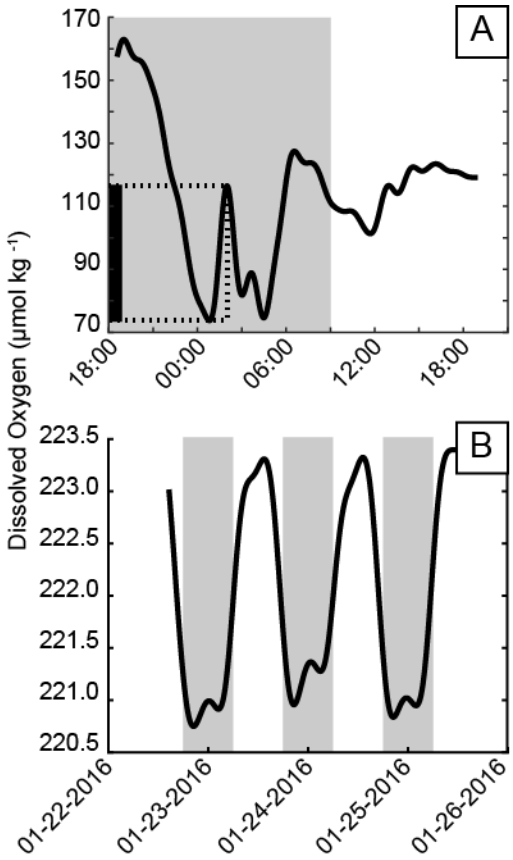

674

675

Tables

Table S1. Location and reference data for global locations of night time dissolved oxygen (DO) spikes in Figure 1.

Number corresponds to the number on Figure 3. Amplitude refers to the average height of the nighttime DO spike, as estimated from the published data. Duration refers to the length of time during which the nighttime DO spike occurred.

Number	Location	Lat	Lon	Date	Amplitude	Duration (h)	Ref.
1	Saca di Goro, Adriatic Sea, Italy	44.47 N	12.15E	1992	50% Sat	4-6	16
2	Long Island Sound, USA	41.14 N	72.77W	2010	5umol/L	~6	31
3	Flax Pond, Long Island Sound, USA	40.58 N	73.82W	2014	2mg/L	4-6	32
4	Onacock Creek, Cheasapeake Bay, USA	37.43 N	75.51W	2008	2mg/L	>3	33
5	South Bay, Virginia, USA	37.15 N	75.48W	2014	100mmol/m^2/d	6-8	18
6	Eilat, Red Sea, Israel	29.33 N	34.57E	1998	78% sat	~6	22
7	Aqaba, Red Sea, Jordan	29.29 N	34.58E	2010	2mg/L	~6-8	34
8	Florida Keys National Marine Sanctuary, USA	25.06 N	80.18W	2013	200 mmol/m^2/d	4	35
9	Florida Bay, Florida, USA	25.03 N	80.37W	2000	200umol/L	4-6	36
10	Bora Bay, Japan	24.45 N	125.20E	1993	50 mmol/L	4	13
11	Bora Bay, Japan	24.45 N	125.20E	1995	25umol/L	4	15
12	Shiraho Reef, Ryukyu Islands, Japan	24.22 N	124.15E	1998	4 mg/L	~4	21
13	Kane'ohe Bay, O'ahu, USA	21.25 N	157.47 W	2012	0.5mg/L	4	37
14	Hainan, China	19.31 N	110.51E	2012	0.5mg/L	~4	17

Number	Location	Lat	Lon	Date	Amplitude	Duration (h)	Ref.
15	Enrique Reef, La Parguera, Puerto Rico	17.57 N	67.03W	2009	20umol/L	~6	38
16	Piscaderabai, Willemstad, Curacao	12.7N	68.56W	2015	2umol/L	6	this study
17	Kingman Reef, Northern Line Islands, USA (territory)	06.24 N	162.24 W	2010	5umol/L	6	this study
18	Palmyra Atoll, Nothern Line Islands, USA (territory)	05.52 N	162.6W	2010	5umol/L	6	this study
19	Palmyra Atoll, Nothern Line Islands, USA (territory)	05.52 N	162.6W	2014	15umol/L	6	this study , 24
20	Teraina (Washington Island), Northern Line Islands, Kiribati	04.43 N	160.24 W	2010	5umol/L	6	this study
21	Tabuaeran (Fanning Island), Northern Line Islands, Kiribati	03.52 N	159.22 W	2010	5umol/L	6	this study
22	Jarvis Island, Southern Line Islands, USA (territory)	00.22S	160.03 W	2013	2umol/L	6	this study
23	Malden Island, Sourthern Line Islands, Kiribati	04.01S	154.59 W	2013	10umol/L	6	this study
24	Starbuck Island, Southern Line Islands, Kiribati	05.37S	151.5W	2013	5umol/L	6	this study
25	Millennium Island, Southern Line Islands, Kiribati	09.57S	150.13 W	2013	15umol/L	6	this study
26	Vostok Island, Southern Line Islands, Kiribati	10.06S	152.25 W	2013	5umol/L	6	this study
27	Flint Island, Southern Line Islands, Kiribati	11.26S	151.48 W	2013	2umol/L	6	this study

Number	Location	Lat	Lon	Date	Amplitude	Duration (h)	Ref.
28	Yonge Reef, Great Barrier Reef, Australia	14.5S	145.6E	1993	40% Sat	6	39
29	Mo'orea, French Polynesia	17.30S	145.0W	1975	1 mg/L	4	14
30	Mo'orea, French Polynesia	17.30S	145.0W	1988	2 mg/L	8	20
31	Mo'orea, French Polynesia	17.48S	149.84 W	2011	50umol/L	6	this study , 23
32	Heron Island, Great Barrier Reef, Australia	23.27S	151.55E	2011	50umol/L	3-4	40
33	Mo'orea, French Polynesia	17.30S	145.0W	1992	0	0	39
34	Shiraho Reef, Ryukyu Islands, Japan	24.22 N	124.15E	2015	0	0	41
35	Tampa Bay, Florida, USA	27.36 N	82.35W	2003	0	0	36
36	San Jacinto Wetland, Texas, USA	29.48 N	95.04W	2004	0	0	42
37	Sugar Creek, Indiana, USA	40.40 N	87.18W	2003	0	0	43
38	Snug Harbor, Cape Cod, USA	41.36 N	70.38W	2013	0	0	44
39	Crystal Lake, Northern Highland Lakes District, USA	46.0 N	89.36W	2003	0	0	45

PeerJ Preprints NOT PEER-REVIEWED

Table S2. Covariance between DO and oceanographic data as detected by Granger causality.

Mo'orea			
Date	**Sensor**	**Causal Direction**	**Wind Speed**
Sept. 8, 2011	3	[var] causes DO	2.89E-02
		DO causes [var]	3.86E-04

Line Islands					
Island	**Sensor**	**Causal Direction**	**Moon Phase**	**Pressure at 300 m below surface**	**Wind Speed**
Flint	6	[var] causes DO	--	4.28E-02	--
		DO causes [var]	--	4.37E-02	--
Millennium	2	[var] causes DO	--	--	1.59E-03
		DO causes [var]	--	--	1.25E-02
Washington	5	[var] causes DO	2.76E-03	--	--
		DO causes [var]	4.05E-03	--	--
	6	[var] causes DO	1.36E-02	--	--
		DO causes [var]	2.43E-02	--	--

Palmyra 2014					
Site	**Causal Direction**	**Temperature**	**pH**	**Salinity**	**Pressure at 0.3 m above the benthos**
LL	[var] causes DO	1.78E-15	3.09E-12	0.00E+00	1.04E-10
	DO causes [var]	6.13E-14	7.41E-05	0.00E+00	2.71E-08

682

683

PeerJ Preprints NOT PEER-REVIEWED

Table S3. Astronomical and meteorological data cannot fully explain the night time dissolved oxygen spikes.

Significant P-values (<0.05) for multivariate Grainger causality analysis of dissolved oxygen time series versus astronomical and meteorological time series data spanning the same time frame as the dissolved oxygen measurements. Only the significant P-values are reported.

Mo'orea					
Date	**Sensor**	**Moon Phase**	**Pressure at Sea Level**	**Wind Speed**	**Wind Direction**
Sept. 1, 2011	1	--	9.35E-03	--	--
Sept. 5, 2011	4	--	--	2.06E-02	3.20E-04
	5	--	1.13E-02	2.93E-03	--
	3	--	--	2.89E-02	--

Line Islands						
Island	**Sensor**	**Moon Phase**	**Pressure at 300 m below surface**	**Pressure at 500m below surface**	**Wind Speed**	**Pressure at 0.3 m above the benthos**
Fanning	3	--	--	2.67E-02	--	ND
	4	--	1.34E-02	1.14E-02	--	ND
Flint	1	4.73E-02	--	1.93E-02	1.03E-06	ND
	2	--	4.15E-02	--	3.37E-03	ND
	3	--	--	9.19E-03	1.79E-08	ND
	4	6.58E-03	--	--	1.60E-04	ND
	5	--	2.12E-02	--	5.18E-04	ND
	6	--	--	--	1.67E-04	ND
Jarvis	5	--	--	--	2.67E-03	ND
Kingman	6	9.78E-04	--	--	--	ND
Malden	4	--	2.94E-02	--	--	ND
Millennium	1	7.58E-05	--	--	1.06E-03	ND
	2	1.06E-03	--	2.23E-03	--	ND
	3	1.83E-03	--	--	--	ND
	4	5.21E-04	--	--	1.53E-02	ND
	5	5.32E-06	--	--	3.90E-02	ND
	6	1.46E-11	--	--	7.94E-03	ND
Palmyra	1	2.58E-02	4.00E-02	4.06E-02	--	ND
	6	1.33E-02	--	--	--	ND
Washington	1	2.98E-03	--	--	--	ND
	2	2.40E-04	--	--	--	ND
	3	4.93E-03	--	--	--	ND
	4	2.22E-04	--	--	4.84E-02	ND
Palmyra (2014)	Site RT4	ND	ND	ND	ND	1.64E-13

PeerJ Preprints NOT PEER-REVIEWED

690

691 Table S4. Sample parameters for *in vitro* benthic incubations.

Tank	Sample Type	Sample Displacement (estimate, mL)	Depth (m)	Location	Amplitude (umol kg^-1)	Duration (hr)
1	Mixed	1000	9	Water Factory	0	0
2	Mixed	1000	9	Water Factory	0	0
3	Sediment	667	9	Water Factory	0	0
4	Mixed	1000	9	Water Factory	0	0
5	Mixed	1333	9	CARMABI	0	0
6	Sediment	1333	9	CARMABI	0	0
7	Mixed	1000	5	San Marie	0	0
8	Sediment	1000	5	Salt Marsh	0	0
9	Mixed	1000	5	Salt Marsh	0	0
10	Turf	1000	5	Salt Marsh	0	0
11	Mixed	1333	9	Water Factory	0	0
12	Sediment	1333	9	Water Factory	0	0
13	Mixed	1000	9	East Point	0	0
14	Mixed	1000	9	East Point	0	0
16	Mixed	1000	9	East Point	0	0
17	Mixed	1000	9	East Point	0	0
18	Mixed	1000	9	East Point	0	0
19	Mixed	1000	9	East Point	0	0
1.2	Rubble	1333	9	Sea Aquarium	0	0
2.2	Rubble	1333	9	Sea Aquarium	0	0
1.3	Turf	1000	9	Water Factory	0	0
2.3	Rubble	1000	9	Water Factory	0	0
1.4	Mixed	1000	9	Water Factory	0	0
2.4	Mixed	1000	9	Water Factory	0	0
3.4	Seawater (control)	2000	9	Water Factory	0	0
4.4	Tap water (control)	2000	N/A	N/A	0	0
1.5	Mixed	1333	9	CARMABI	0	0

1.6	Sediment	667	1	CARMABI	0	0
1.7	Mixed	1000	10	Water Factory	0	0
2.7	Mixed	1000	10	Water Factory	0	0
3.7	Mixed	1000	10	Water Factory	0	0
1.8	Turf	1333	5	Water Factory	0	0
2.8	Mixed	1333	10	Water Factory	0	0
3.8	Mixed	1333	10	Water Factory	0	0
4.8	Turf	1333	5	Water Factory	0	0
1.9	Mixed	1333	10	Water Factory	0	0
2.9	Mixed	1333	10	Water Factory	0	0
3.9	Mixed	1333	10	Water Factory	0	0
4.9	Mixed	1333	10	Water Factory	0	0
5.9	Mixed	1333	10	Water Factory	0	0
1.10.	Turf	115	6	San Marie	0	0
2.10.	Turf	115	6	San Marie	0	0
3.10.	Turf	115	6	San Marie	0	0
4.10.	Turf	115	6	San Marie	0	0
1.11	Sediment	192	12	Water Factory	0	0
2.11	Sediment	500	12	Water Factory	0	0
3.11	Sediment	192	5	Water Factory	0	0
4.11	Sediment	500	5	Water Factory	0	0
5.11	Turf	1000	9	Water Factory	0	0
1.12	Turf	200	12	Water Factory	0	0
2.12	Turf	1000	12	Water Factory	0	0
3.12	Turf	200	5	Water Factory	0	0
4.12	Turf	1000	5	Water Factory	0	0
5.12	Rubble	1333	10	Water Factory	0	0
1.13	Turf	200	5	Water Factory	0	0
2.13	Turf	200	5	Water Factory	0	0
3.13	Turf	200	5	Water Factory	0	0
4.13	CCA	200	5	Water Factory	0	0
5.13	Dry rubble (control)	1000	Intertidal	Water Factory	0	0

PeerJ Preprints NOT PEER-REVIEWED

1.14	Rubble	200	12	Water Factory	0	0
2.14	Rubble	200	12	Water Factory	0	0
3.14	Seawater (control)	2000	Surface	Flow-through System	0	0
4.14	Rubble	1000	12	Water Factory	0	0
1.15	Turf	200	9	Water Factory	0	0
2.15	Turf	200	9	Water Factory	0	0
3.15	Rubble	1000	9	Water Factory	0	0
4.15	Rubble	1000	9	Water Factory	0	0
5.15	Turf	1000	9	Water Factory	0	0
1.16	CCA	200	12	Water Factory	0	0
2.16	CCA	200	12	Water Factory	0	0
3.16	CCA	500	12	Water Factory	60	4 - 5
4.16	CCA	200	12	Water Factory	0	0
1.17	CCA	500	Intertidal	CARMABI	100	3
2.17	CCA	500	Intertidal	CARMABI	0	0
3.17	CCA	500	Intertidal	CARMABI	0	0
3.18	CCA	500	12	Water Factory	0	0
4.18	CCA	500	12	Water Factory	0	0
5.19	CCA	500	12	Water Factory	0	0

692

PeerJ Preprints NOT PEER-REVIEWED

Table S5. Description of Birch Aquarium tanks used in this study

Tank Number	L x W x D (m)	Volume(L)	Sump Volume(L)	Bio-filtration	Mechanical Filtration	Chemical Additions	Protein Skimming	Lighting	Light Cycle	Natural Seawater Additions	Pump Flow Rate	Notes
26	2.5X1.5X1.2	4,270	765	Live rock	4 - 100um filter socks	Calcium reactor	Yes	3 - 1K watt metal halide bulbs; 2 - 54 watt T5 Actinic 03 bulbs; Some sunlight in spring-summer	0700-1900	Yes, ~2L/min, 24h/day	130-150L/min, with flow eductors~550L/min	
27	2.8X1.5X1.3	4,542	200	Live rock	1 - 100um filter sock	None	Yes	2 - 1K watt metal halide bulbs	0700-1900	Yes, ~4L/min, 24h/day	~70-100L/min	Semi circular shaped tank - measurements provided are greatest length, width
31	1.5X1.1X1.1	946	No sump	Live rock	None	None	None	1 - 250 watt metal halide bulb	0830-1730	Yes ~1L/min, 24h/day	1 submersible pump, Approx. 190L/min	Hexagonal tank. Measurements provided are greatest width and length
15a	1.5X0.9X0.6	776	212	Live rock	None	None	Yes	2 - 250 watt metal halide bulbs; 2 - 54 watt T5 fluorescent bulbs	0700-1830	Yes ~3L/min, 24h/day	2 Submersible pumps, Approx. 1100L/min	
15b	2.4X0.8X0.4	757	212	Live rock	None	None	Yes	2 - 234 watt T5 flourescent bulbs	0700-1830	Yes ~3L/min, 24h/day	2 Submersible pumps, Approx. 1100L/min	

693